CHAPTER 3

A Mathematical Examination of Multiple Asymmetric Transformations:

Statistical Amplification and the Horeau Principle.

3.1 INTRODUCTION

Multiple asymmetric transformations are powerful reactions that establish multiple stereocenters in a single synthetic transformation. The ability to sequentially and selectively execute more than one bond-forming event in a single operation is undeniably advantageous to any complicated multistep synthesis. In addition to the expediency gained in bond construction, this technique also holds the potential to impart beneficial amplification to the enantiomeric purity of the terminal product. However, whereas the course of solitary enantioselective transformations are very well understood, the impact of more than one such reaction upon a single substrate is typically more complicated. This is particularly true with regard to prediction and analysis of the eventual enantio- and diastereomeric enrichment of the final product. The following chapter examines the impact of compound dimerization events and multiple asymmetric transformations with a specific focus on the stereochemical outcome of these reactions, as well as the possible

pathways relevant to the course of these reactions. The nature of statistical amplification and its benefits in complex molecular synthesis are explored mathematically and empirically, with particular attention paid to the effect known as the Horeau Principle.

3.1.1 PRELIMINARY RESULTS AND INITIAL INTEREST

Recently, our group completed the total synthesis of the marine diterpenoid natural product cyanthiwigin F.[1] Vital to the success of our synthetic route was the use of an early-stage double asymmetric catalytic alkylation reaction to simultaneously set two all-carbon quaternary stereocenters.[2] By subjecting bis(β-ketoester) (**186**) to a catalyst comprised of palladium(0) and (*S*)-*t*-BuPHOX (**193**), it was possible to realize the synthesis of diketone (*R*, *R*)-**185** in 78% yield, with an exceptional *ee* of 99% and a dr of 4.4:1 (Scheme 3.1). While we were delighted to obtain such a high level of enantioselectivity, the modest diastereomeric ratio observed in this reaction was not anticipated. Our experience concerning the catalytic enantioselective alkylation of isolated, single β-ketoester substrates routinely yielded products with roughly 95 : 5 selectivity. As such, it was our expectation that the double stereoselective alkylation would afford the desired product with a high level of diastereoselectivity. Indeed, because the reaction was selective to the point of affording essentially enantiopure (*R*,*R*)-**185**, we anticipated that the process would also strongly favor the formation of C_2 symmetric isomer (*R*,*R*)-**185** over the *meso* diastereomer of diketone **185**.

Scheme 3.1 Double asymmetric catalytic alkylation

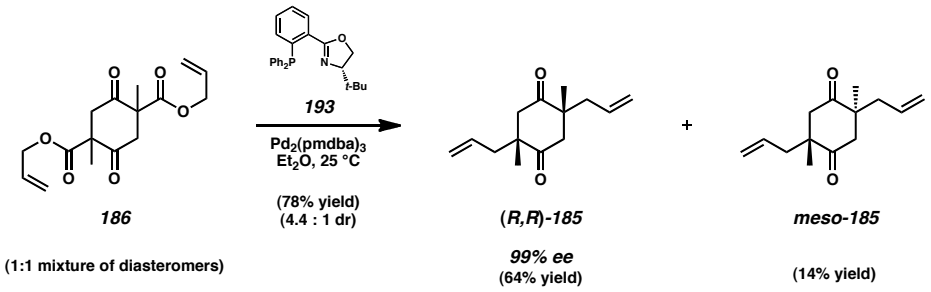

In order to examine other cases of double asymmetric alkylation, we desired to develop alternative substrates with which to probe these processes. Though bis(β-ketoester) **186** had proven to be an efficient substrate for the synthesis of the cyanthiwigin natural products, the nature of its preparation obviated the potential to efficiently separate the primary and secondary alkylation processes. Therefore, we sought a different class of double alkylation substrate that, with appropriate substitution, would allow the two alkylation steps to be cleanly and predictably differentiated from one another. For example, carbonate (±)-**223** was designed specifically as a substrate for such a double allylation reaction (Scheme 3.2).[3] Not only does ester **223** contain a reactive enol carbonate functionality, but it also boasts a latent β-ketoester moiety, a group that is only revealed upon conclusion of the first alkylation process. Treatment of enol carbonate **223** with palladium(0) and ligand **193** provided smooth access to cyclohexanone **224** in 76% yield and 92% *ee*. However, just as the case of bis(β-ketoester) **224** the diastereomeric ratio of C_2 symmetric ketone (*S*,*S*)-**224** to *meso* ketone **224** was mediocre (4.0 : 1).

Scheme 3.2 Double asymmetric catalytic alkylation of an enol carbonate ester substrate

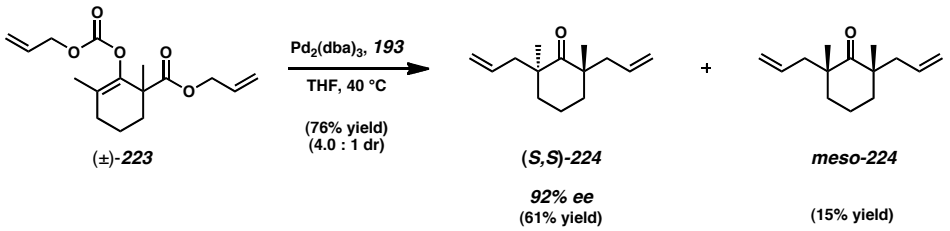

With these results in hand, we reasoned that optimization of the diastereomeric ratio resulting from these transformations would require a deeper understanding of the course of the reaction. Toward this end, we became interested in thoroughly scrutinizing the selectivity of alkylation at each independent C–C bond-formation step for any given double stereoselective process. Ideally, we sought a method to determine these desired selectivity values from the three observable stereochemical values of the final product of a double stereoselective transformation, namely the diastereomeric ratio (dr) and the enantiomeric excess of both isolated diastereomers (ee_A and ee_B).[4] As we quickly came to understand, a thorough investigation of multiple asymmetric processes required a historical review of the literature, as well as a mathematical representation of the stereoisomers involved.

3.2 DUPLICATION AND MULTIPLE ASYMMETRIC PROCESSES

The following sections investigate the historical and mathematical aspects of statistical amplification as it relates to both duplication reactions and multiple asymmetric transformations. A brief history of scalemic dimerization is followed by a presentation of the pertinent equations related to this phenomenon. The same treatment is then given to multiple asymmetric reactions, with a specific focus on double asymmetric processes.

3.2.1 THE HISTORY OF STATISTICAL AMPLIFICATION

The fundamental concepts related to the statistical amplification of enantiomeric excess in multiple asymmetric reactions were first investigated in relation to non-enantioselective transformations. Indeed, one of the earliest reported examples of this enantioenrichment phenomenon utilized no external chiral reagents whatsoever, but instead involved the dimerization of a scalemic mixture of starting materials.

In 1936, Langenbeck and coworkers conducted a series of experiments in an effort to understand the mechanisms maintaining the enantiopurity of naturally occurring compounds.[5] He observed that "with every synthesis of an optically active compound from inactive starting materials, a degradation in optical purity takes place; that is, the newly formed compound is less optically active than the compound from which the optical activity was derived." Langenbeck further elaborated his postulate by explaining that, "If an enzyme is synthesized using another optically active enzyme, the newly formed product cannot be optically pure. The infinite repetition of these processes over a geological time period would have led to a complete loss of optical activity in enzymes (and therefore of all naturally occurring compounds) if the degradation in optical purity were not compensated for by an increase in optical purity in a different process."[5]

In order to seek out and study this enantiopurity preservation process, Langenbeck and coworkers subjected multiple samples of L-menthol (L-**225**) (each with varying degrees of enantioenrichment) to a process of dimerization with oxalyl chloride (**226**, Scheme 3.3A). Upon measuring the optical rotation of the resulting dimers (**227**) obtained from increasingly enantiopure samples of alcohol L-**225**, nonlinear deviations were observed that did not match the expected behavior (Scheme 3.3B). Curve I depicts

the optical rotation measured for the individual samples of L-menthol employed, while curve II represents the optical rotation of the resulting dimer formed from each of these samples. In nearly every instance, Langenbeck observed that the optical rotation of the dimer was significantly different than the optical rotation of the corresponding menthol monomer employed. Repetition of this experiment while employing modern HPLC techniques has verified that the *ee* of the dimer is greater than that of the starting material for every experiment run.[5b]

*Scheme 3.3 (A) Langenbeck's initial experiment (B) Curves depicting the optical rotation of samples of (I) L-**225** and (II) **227** vs enantioenrichment of L-menthol starting material*

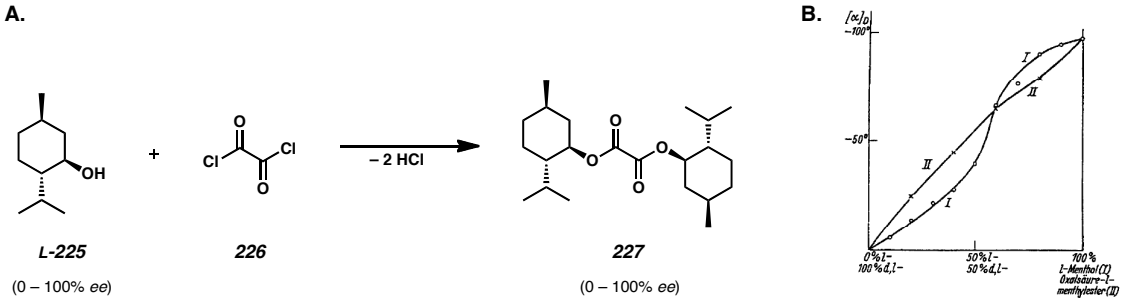

The amplification in enantiopurity measured in the product dimers when compared to their relative starting materials was puzzling. Because no enantioenriched materials beyond L-menthol (L-**225**) were employed in the reaction, it was not immediately clear how the *ee* of the product obtained could exceed that of the starting material used. To rationalize this observation, Langenbeck concluded that the increase in observed *ee* of the product must be the result of a statistical phenomenon.

If one examines the course of this transformation, initial reaction of a scalemic mixture of L-menthol (L-**225**) with oxalyl chloride (**226**) would necessarily produce intermediate acid halide species (*R*,*R*,*S*)-**228** (Scheme 3.4). Depending on the level of

enantiopurity of the menthol used in this reaction, some quantity of D-menthol (D-**225**) would be present in the reaction mixture, and thus would be expected to react in a corresponding manner to give acid halide (*S*,*S*,*R*)-**228**. Intermediate acid chlorides (*R*,*R*,*S*)-**228** and (*S*,*S*,*R*)-**228** would then undergo reaction with an additional equivalent of either L- or D-menthol, ultimately producing one of three stereoisomeric products. In the event that either ester (*R*,*R*,*S*)-**228** or ester (*S*,*S*,*R*)-**228** react with another molecule of menthol of the same enantiomeric sense as the first reaction, then homochiral isomers (L,L)-bis-menthyl oxylate (L,L-**227**) or (D,D)-bis-menthyl oxylate (D,D-**227**) will result. If either intermediate (*R*,*R*,*S*)-**228** or (*S*,*S*,*R*)-**228** react instead with the opposite enantiomer of menthol, the heterochiral (*meso*)-bis-menthyl oxylate (*meso*-**227**) will be afforded.

Scheme 3.4 Product pathways for Langenbeck's duplication experiment

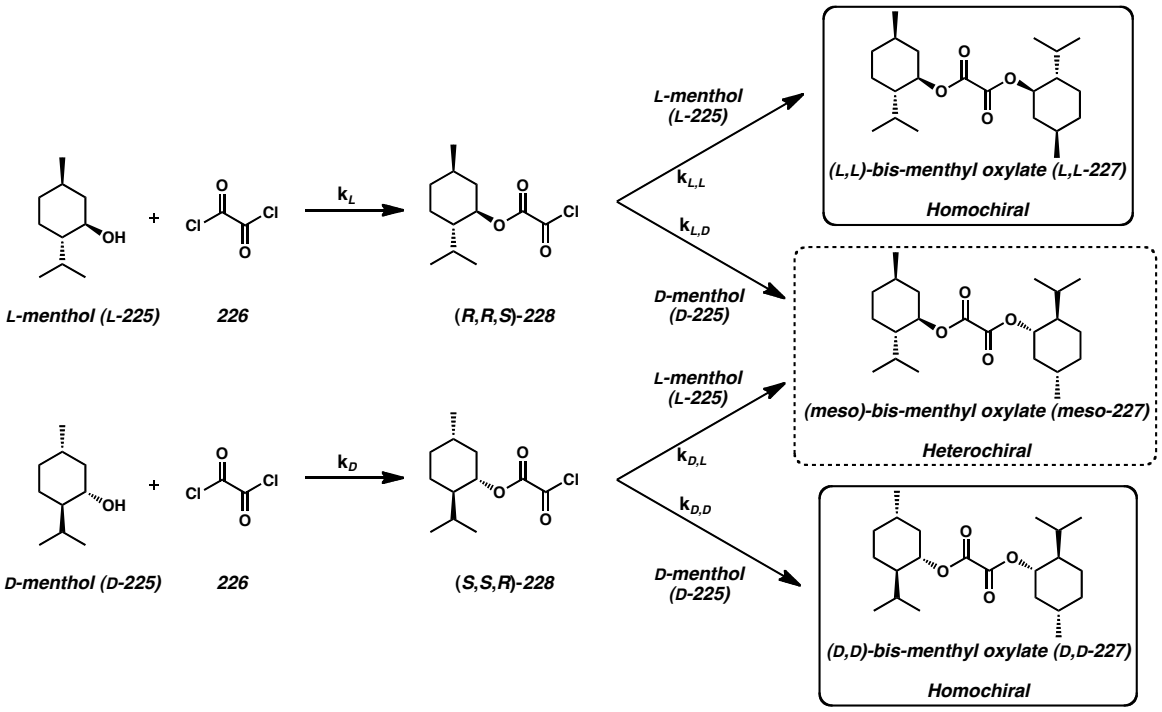

At the time of his initial experiment, Langenbeck surmised that the observed deviation in optical purity was a consequence of the distribution between the diastereomers formed as the eventual reaction products. Because the *meso* diastereomer is composed of one D- and one L-isomer of menthol, and because this diastereomer cannot rotate polarized light, the formation of this dimer in Lagenbeck's experiment effectively represented the removal of racemic menthol from the observable system. Though he had no way to effect the physical separation of these diastereomers, Langenbeck nevertheless hypothesized that "If it were possible to separate the *meso* ester quantitatively, then it would be expected that even with the use of L-menthol with a low *ee* value, an increase in the optical purity of the product would be observed."[5]

Over 40 years after the publication of Langenbeck's findings, Horeau and coworkers revisited the concept of enantiomeric amplification via duplication.[6] With the benefit of improved purification techniques, Horeau was able to perform his own dimerization experiments in order to further elucidate the nature of this phenomenon. Using a system similar to the dimerization of L-menthol, Horeau *et al*. investigated the reaction of scalemic *sec*-phenethyl alcohol (**229**, 60% *ee*) with diethyl carbonate under alkaline conditions (Scheme 3.5).

Scheme 3.5 Duplication of sec*-phenethyl alcohol by Horeau*

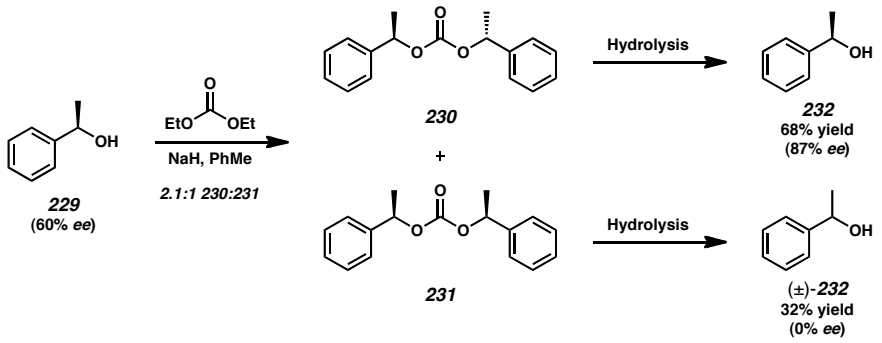

Dimerization of *sec*-phenethyl alcohol (**229**) afforded both the homochiral carbonate **230** and the heterochiral carbonate **231**, in a 2.1 : 1 ratio. After purification, separation, and hydrolysis of these diastereomeric products, two different samples of *sec*-phenethyl alcohol were isolated.[7] The alcohol product **232** obtained from the heterochiral diastereomer (**231**) was observed to be completely racemic, whereas saponification of the homochiral diastereomer (**230**) afforded enantioenriched alcohol **232** in 87% *ee*. This result represented a statistical amplification of *ee* without the use of external chiral reagents, as *sec*-phenethyl alcohol was enriched by 27% *ee* via simple dimerization of the starting material. These results experimentally confirmed Langenbeck's previous hypothesis, as the duplication process effectively allowed for the removal of racemic substrate via the separation of diastereomeric intermediates.

3.2.2 MATHEMATICAL REPRESENTATION OF HOREAU DUPLICATION

In order to extrapolate his experimental findings into a useful, predictive model, Horeau subsequently addressed the duplication phenomenon from a mathematical perspective. For any scalemic material for which one arbitrarily assigns that the *R*

enantiomer (**233**) predominates over the *S* enantiomer (**234**), the relative mol fraction of the two isomers is represented by x for the *R* enantiomer and 1 – x for the *S* enantiomer (Scheme 3.6A). If the possible reactive pathways toward complete dimerization are followed, reaction of either enantiomer with a dimerization linker (**235**) will afford either the *R*-substituted (**236**) or *S*-substituted (**237**) intermediate. Further reaction of these intermediates with the remaining monomeric components thereafter furnishes the expected dimers in four different stereoisomeric forms. The *R*-derived intermediate **236** can further react with either enantiomer of the starting material to furnish the homochiral (**238**) or the heterochiral (**239**) diastereomer. Similarly, the *S*-derived intermediate **237** can also produce heterochiral (**240**) and homochiral (**241**) products.

If a number of assumptions are applied to this system, two very useful equations can be applied to the duplication phenomenon. The reaction pathways illustrated below contain six different transformations, each with its own distinct rate constant. In order for the obtained mathematical representations to be manageable, it is assumed that all six of these rate constants are reasonably similar ($k_R \cong k_S \cong k_{RR} \cong k_{RS} \cong k_{SR} \cong k_{RR}$). This precludes the possibility of kinetic resolution at any point in the reaction process, and additionally presumes that no chiral recognition or asymmetric induction occurs between the chiral intermediates **236** or **237** and the monomeric starting materials **233** and **234**. Although this assumption may appear at first to be extreme, if the nature of the dimerization linker **235** is such that the two reactive centers are sufficiently removed from one another, these simplifications become quite appropriate. Additionally, all reactions are assumed to proceed to completion, so that all molecules of starting material (**233** and **234**) and intermediate (**236** and **237**) are consumed in this process.

Scheme 3.6 (A) Reaction pathways for Horeau-type dimerization and (B) mathematical representations of relevent stereoisomeric quantities

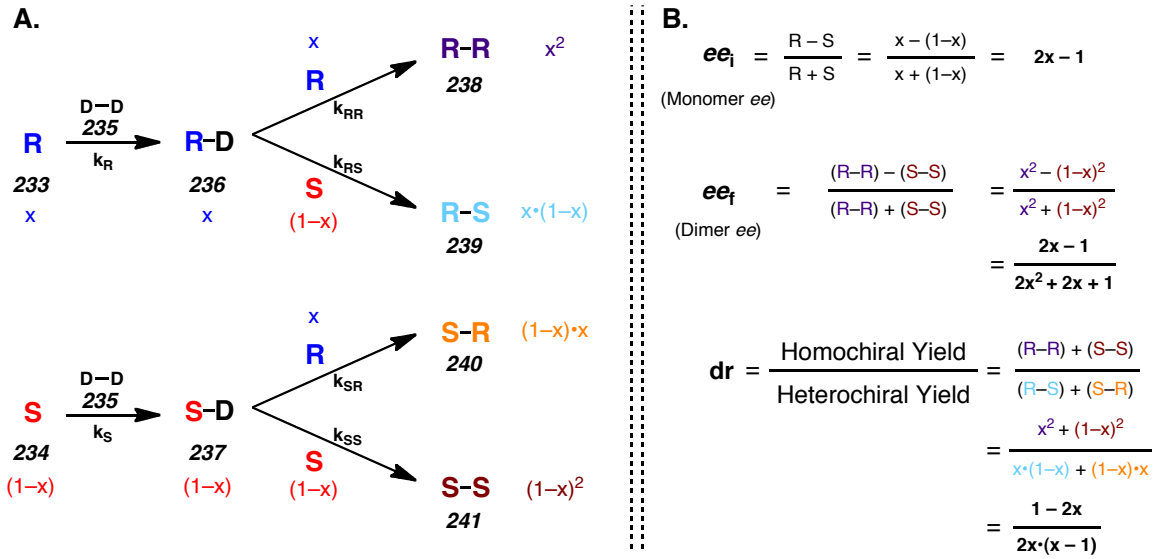

With these assumptions in place, it is possible to leverage the expressions for the mol fraction of the starting material *R* and *S* enantiomers in order to derive expected yields for all four stereoisomers of product. These values can thereafter be used in expressions for the diastereomeric ratio and enantiomeric excess of the product mixture (Scheme 3.6B). By exploiting the relationship between the mol fraction of the major enantiomer (x) and the initial enantiomeric excess of the scalemic starting material ($ee_i = 2x - 1$), further substitution and manipulation provide two simple and extremely useful expressions for the diastereomeric ratio (dr) and enantiomeric excess (ee_f) of the product dimer.

$$dr = \frac{1 + (ee_i)^2}{1 - (ee_i)^2} \quad (1) \qquad ee_f = \frac{2 \cdot ee_i}{1 + (ee_i)^2} \quad (2)$$

Though these equations are greatly simplified due to the assumption of rate equivalence, they nevertheless provide valuable insight into the behavior of enantiomeric amplification in Horeau-type duplications. After converting equation (1) from a

relationship in terms of diastereomeric ratio into an expression representing diastereomeric excess, it is possible to plot the final dimer enantiomeric excess (ee_f) and diastereomeric excess (*de*) of the product dimer versus the initial enantiomeric excess of the scalemic starting material (ee_i).[8] Additionally, the total yield of the heterochiral diastereomer as it relates to ee_i can also be calculated (Figure 3.1). As expected, the value of ee_f displays a rapid and positive nonlinear deviation when compared to the ee_i value of the starting material. Indeed, even with an initial ee_i as low as 50%, an enantiomeric excess of roughly 80% is predicted for ee_f after duplication, a value that represents a considerable increase in enantioenrichment.

In addition to the obvious gains imparted by this technique, these equations also illustrate the inherent cost of Horeau-type duplication. The value for diastereomeric excess increases much more slowly relative to the value of ee_f for similar increases in ee_i. This pronounced negative nonlinear deviation represents the quantity of racemic starting material separated from the mixture in the form of the heterochiral diastereomer (For example, **239** and **240**, Scheme 3.6). Hence, any duplication technique of this type necessarily incurs a synthetic penalty, in that the overall yield of enantioenriched material obtained will be negatively impacted. For example, the case of a 50% value for ee_i would afford the homochiral diastereomer in approximately 80% ee_f. However, this same reaction would also generate a diastereomeric ratio of 1.7 : 1 dr (25% *de*). These results correlate to roughly 37% of the original scalemic material that must be sacrificed in order to achieve enantioenrichment. Despite this drawback, Figure 3.1 clearly illustrates that for larger values of ee_i the benefits of Horeau-type duplication remain high, while the costs in terms of yield become vanishingly small.

Figure 3.1 A graphical representation of the impact of Horeau duplication

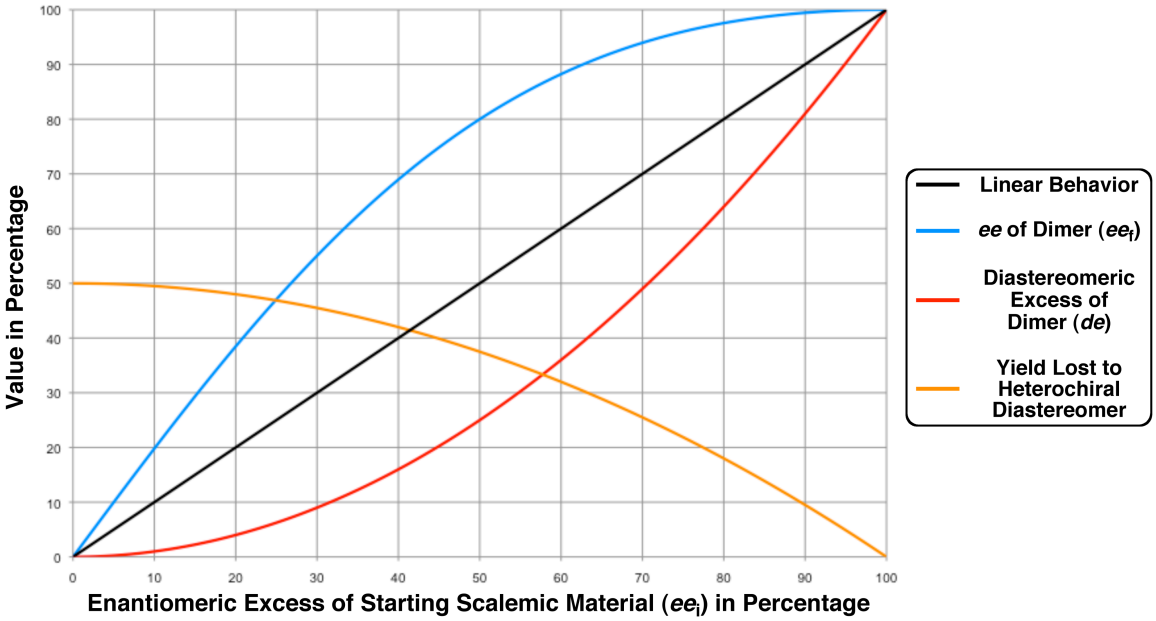

Encouragingly, application of these equations to Horeau's experimental duplication of *sec*-phenethyl alcohol is in excellent agreement with the observed data. For starting material of 60% ee_i, the expressions (1) and (2) afford values for ee_f and dr of 88% and 2.13:1, respectively. When compared to the physically determined values of 87% ee_f and 2.10:1 dr, the approximations above appear to be quite reasonable in predicting the outcome of simplistic dimerizations.

Overall, Horeau-type duplications are a useful way to approach the enantioenrichment of a scalemic mixture without requiring traditional chiral resolution techniques. Provided that no chiral recognition or asymmetric induction occurs during dimerization, these reactions provide a very quick route toward exceptional ee_f values by sequestering racemic material within a heterochiral diastereomer. This undesired material can then be separated from the homochiral diastereomer via traditional purification methods to impart enantioenrichment. However, it should always be noted

that the removal of the heterochiral diastereomer incurs a synthetic penalty in the form of lost yield, and the dr of Horeau-type duplications are typically sluggish to increase to acceptable levels.

3.2.3 SYNTHETIC APPLICATIONS OF THE HOREAU DUPLICATION

In the time since Horeau's explanatory report concerning duplication as a method for enantioenrichment, this technique has been used to approach numerous synthetic problems. For instance, the non-linear behavior of these duplication events provides an expedient and transparent method for the excellent enantioenrichment of scalemic intermediates in the course of a complex natural products synthesis.

One notable example of this phenomenon can be found in the total synthesis of the carpenter bee hormone 2,8-dimethyl-1,7-dioxaspiro[5.5]undecane (**247**), and the controversy surrounding its preparation. In 1981, Mori and coworkers reported the preparation of this particular bee hormone from ethyl acetoacetate (**242**, Scheme 3.7).[9] Their synthesis leveraged a reduction of ketone **242** via the action of baker's yeast to afford enantioenriched 3-hydroxy-butanoate (**243**) in 92% *ee*. This material was thereafter advanced several steps to protected iodide substrate **244**.

Scheme 3.7 Initial steps toward Mori's synthesis of 2,8-dimethyl-1,7-dioxaspiro[5.5]undecane

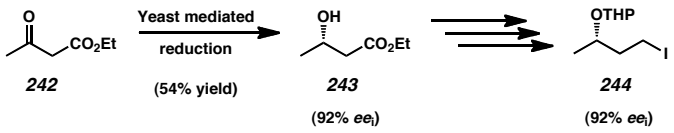

With iodide **244** in hand, Mori *et al*. were then able to complete the total synthesis of 2,8-dimethyl-1,7-dioxaspiro[5.5]undecane by leveraging a Horeau-type duplication. Treatment of ethyl acetoacetate (**242**) under strongly alkaline conditions was thereafter followed by exposure to enantioenriched iodine **244** (Scheme 3.8). Coupling of these two fragments proceeded smoothly to give β-ketoester **245**, which was subsequently alkylated with a second equivalent of iodide **244**. After saponification and decarboxylation, an acidic workup served to remove of both the alcohol protecting groups and furnish diol **246**. However, before ketone **246** could be isolated, this compound spontaneously underwent spiroacetal formation, thus generating the desired natural products **247** and **248**.

Scheme 3.8 Horeau duplication in Mori's bee hormone synthesis

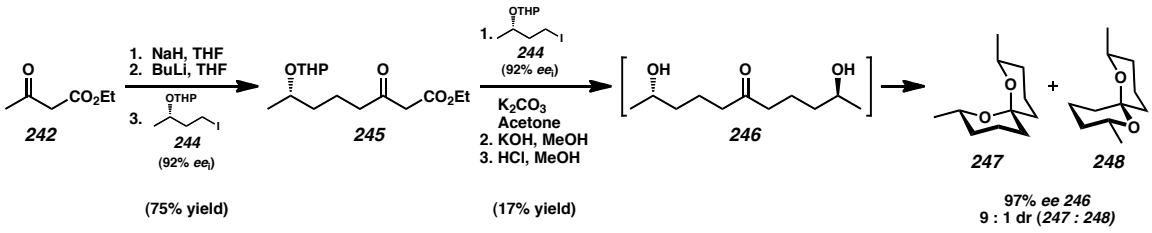

Despite having begun the synthesis with material of 92% ee_i, the Horeau-type dimerization of **244** onto **242** afforded the final natural product in an amplified 97% ee_f and a 9:1 ratio of **247** to **248**. If the initial value of 92% ee_i is substituted into both equations (1) and (2), the final calculated values of 99% for ee_f and 12 : 1 for dr are within acceptable agreement with the experimental data. Nevertheless, the increased ee_f observed by Mori later became a point of dispute. In 1984 Isaksson *et al*. contested the validity of Mori's reported optical rotation values for acetal **247** on the grounds that the

starting iodide **244** was not enantiopure.[10] In order to address these concerns, Mori revisited the synthesis of the hormone **247** using two different samples of iodide **244**, one of which was enantioenriched to 100% ee_i and the other possessing an ee_i of only 85% (Table 3.1). While the enantiopure approach confirmed the optical rotation values reported in Mori's initial synthesis, the lower ee_i sample once again confirmed the Horeau-type duplication phenomenon. With an ee_i of 85% for iodide **244**, the ee_f and dr observed for hormone **247** were 97% and 6.4:1, respectively. Once again, these values are in very good agreement with predictions based on equations (1) and (2).

Table 3.1 Stereochemical summary of Mori's synthetic efforts

ee_i of *244*	Experimentally Determined		Calculated, Predicted Values	
	ee_f of *247*	dr of *247 : 248*	ee_f of *247*	dr of *247 : 248*
85%	97%	6.4:1	99%	6.2:1
92%	99%	9:1	99%	12:1
100%	100%	N/A	100%	N/A

Another example of the Horeau-type duplication approach to enantioenrichment in total synthesis can be found in Corey's preparation of the lignan natural product (–)-wodeshiol.[11] Starting from bromoenone **249**, enantioselective 1,2-reduction of the carbonyl moiety afforded the desired allylic alcohol in high yield, but in only 88% ee_i (Scheme 3.9). Further functionalization of vinyl bromide **250** via lithium-halogen exchange and trapping with chlorotributylstannane provided access to vinyl stannane **251**. This material was subsequently dimerized under palladium–catalyzed homocoupling conditions to generate dimer **252**. Notably, this bis-allylic alcohol was isolated in 99% ee_f and 8.0:1 dr, an impressive enantioenrichment that can be attributed to the statistical amplification of dimerization. Both of these values are predicted

extremely well by equations (1) and (2) based on an 88% value for ee_i. In this particular example, the yield lost to the undesired heterochiral diastereomer is roughly 10%, a value low enough to make the sacrifice synthetically viable. From this point, Corey *et al*. were able to easily complete the total synthesis of (–)-wodeshiol (**253**).

Scheme 3.9. Corey's total synthesis of (–)-wodeshiol via Horeau-type duplication

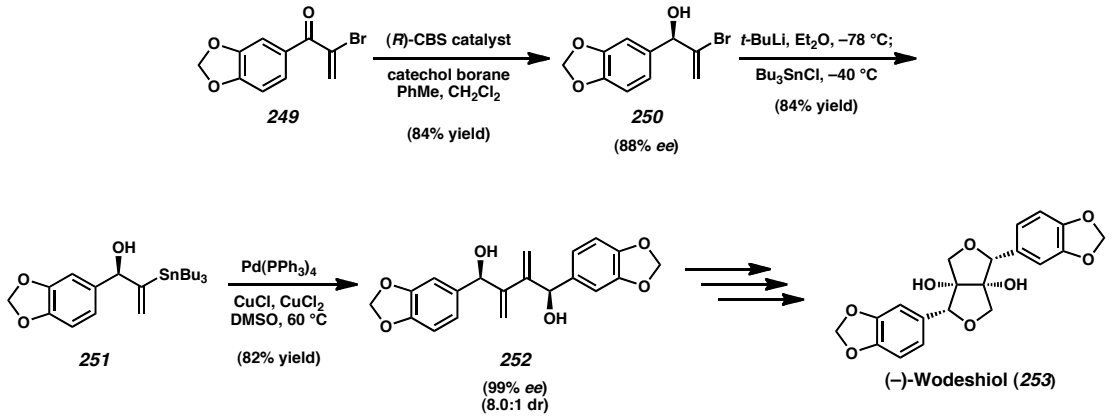

Though Horeau-type duplications have found much application in the direct enantioenrichment of synthetic intermediates, this phenomenon has also been employed toward many other purposes. This technique has facilitated the synthesis of ligands and reagents for further enantioselective synthesis,[12] served as an alternative to traditional resolution with chiral reagents,[13] enabled the development of new analytical methods for the ^{1}H NMR analysis of reagent enantiopurity,[14] and facilitated prediction of the selectivity of an enantioenriched catalyst from its racemic mixture.[15]

The dimerization of scalemic mixtures is an efficient method for the enantioenrichment of modest *ee* material. Provided that the dimerization technique employed obviates the possibility of chiral recognition or kinetic resolution, the outcome of such a reaction can be understood as a consequence of statistical distribution, and thus

can be predicted with simple expressions. However, Horeau-type duplication is not a method of enantioinduction, as all chirality must necessarily be present prior to the dimerization event. Far more complicated are those processes that involve multiple asymmetric transformations.

3.2.4 MULTIPLE ASYMMERTRIC TRANSFORMATIONS

Rather than simply joining two enantioenriched fragments onto a central molecule, multiple asymmetric transformations are processes that construct more than one asymmetric center in a single operation. For example, the interaction of an achiral substrate bearing two prochiral reactive sites with a chiral substrate or a chiral catalyst has the potential to forge four stereoisomeric products in one synthetic process. These transformations hold the potential to efficiently construct multiple key bonds with a high degree of selectivity. Such reactions can also be valuable under circumstances where the desired stereocenters are considerably distal from one another, a circumstance that renders the intramolecular relay of stereochemical information from one stereocenter to a prochiral reactive group quite difficult.

Unfortunately, despite their myriad benefits, multiple asymmetric transformations are significantly more complex than those corresponding reactions that forge a single stereocenter. Indeed, it can be quite difficult to troubleshoot or optimize a multiple asymmetric transformation, due to convoluted reaction pathways and unpredictable substrate-catalyst interactions. Additionally, a rigorous mathematical model of such processes can quickly become overwhelming, a fact that often renders predictive models either cumbersome or inaccessible. Despite these complications, it is possible, via the

application of reasonable assumptions and simplifications, to arrive at expressions for the prediction and analysis of stereoisomeric distributions in these transformations.

In 1994, Kagan *et al*. published an impressively thorough mathematical treatment of double enantioselective transformations.[16] In order to illustrate the numerous variables involved in multiple asymmetric catalysis, Kagan considered the reaction of an enantioselective hydrogenation catalyst with a single molecule bearing two distinct, prochiral olefin moieties. Starting from completely achiral bis-olefin [1*P*, 2*P*] (**254**), complete reaction at both prochiral sites would yield two diastereomeric products (hereafter referred to as diastereomer A and diastereomer B), with each diastereomer possessing a distinct *ee* value (ee_A and ee_B, respectively, Scheme 3.10).[17] In terms of the course of this reaction, hydrogenation can initially occur at either olefin (1) or olefin (2).[18]

For the case where initial hydrogenation transpires at olefin (1), two enantiomeric intermediates are generated prior to subsequent reduction of olefin (2). If catalyst selectivity is large enough to ensure a non-racemic product, the intermediate [1*R*, 2*P*] (**255**) will predominate over the unfavored [1*S*, 2*P*] (**256**) isomer. In order to gauge the efficacy of this first bond-forming transformation, the value "r" is introduced as a measure of relative selectivity for this reaction to produce **255** relative to **256**. Closely mirroring *ee* in structure, the r term represents the local selectivity of the first transformation only, and varies in size from zero to one. A value of zero denotes a complete lack of selectivity in the reaction, and value of unity signifies exclusive generation of the [1*R*, 2*P*] (**255**) isomer.

Scheme 3.10 Pathways for double asymmetric transformation, route 1

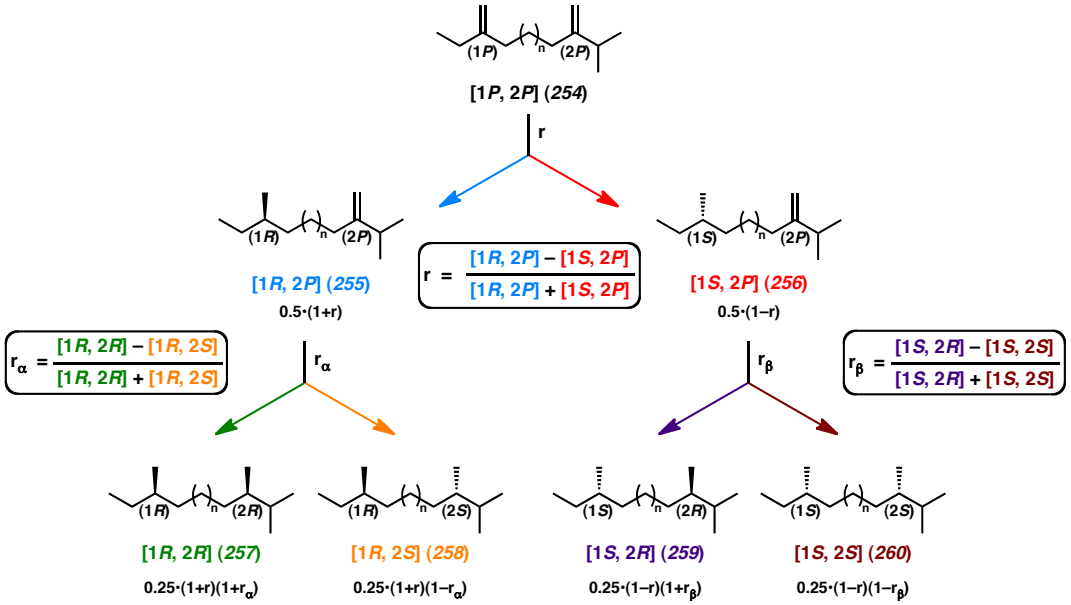

If the reaction is followed further forward, both intermediates **255** and **256** possess one enantioenriched and one reactive prochiral site. Because of this, any additional interaction with the enantioselective catalyst necessarily involves the formation of a diastereomeric catalyst-substrate complex. Thus, in order to fully represent the course of this reaction, two additional selectivity values must be considered, one for either of these possible complexes. Toward this end, the value r_α represents the relative selectivity for formation of the [1*R*, 2*R*] isomer (**257**) over the [1*R*, 2*S*] (**258**) stereoisomeric product starting from the [1*R*, 2*P*] (**255**) intermediate. Similarly, the r_β variable describes the same relationship between [1*S*, 2*R*] (**259**) and [1*S*, 2*S*] (**260**) molecules, as products from the [1*S*, 2*P*] (**256**) intermediate.

It is critical to note that the values for intermediates [1*R*, 2*P*] (**255**) and [1*S*, 2*P*] (**256**) do not reflect isolated yields of the compounds generated in this reaction. Instead, these variables represent the relative quantities of material that pass through each of these

intermediates on the path toward the final products. Additionally, the values [1*R*, 2*R*] (**257**), [1*R*, 2*S*] (**258**), [1*S*, 2*R*] (**259**), and [1*S*, 2*S*] (**260**) represent the quantities of these compounds afforded via route 1 only, rather than the combined total yields of these isomers from the final reaction.

The possibilities explored above (Scheme 3.10) outline the routes that lead to all potential stereoisomeric products in this envisioned reaction. Both products [1*R*, 2*R*] (**257**) and [1*S*, 2*S*] (**260**) contribute to the yield of diastereomer A, and their relative quantities dictate the value ee_A. Similarly, products [1*R*, 2*S*] (**258**) and [1*S*, 2*R*] (**259**) add to the total yield of diastereomer B, and their relative quantities contribute to ee_B. However, the three final values of dr, ee_A, and ee_B cannot be determined from these variables alone. Whereas the situation considered above (Scheme 3.10) initiates with the enantioselective hydrogenation of olefin (1), the possibility also exists that the overall reaction commences with the reduction of olefin (2) (Scheme 3.11). In this situation, the initial intermediates [1*P*, 2*R*]' (**261**) and [1*P*, 2*S*]' (**262**) provide distinct diastereotopic prochiral reactive sites for further enantioselective reduction, which are unique from those intercepted in route 1. As such, a further three selectivity terms are required in order to address the complete set of stereochemical paths available to this reaction. These additional terms (defined as r', r_α', and r_β') are analogous to their route 1 counterparts above.

Scheme 3.11 Pathways for double asymmetric transformation, route 2

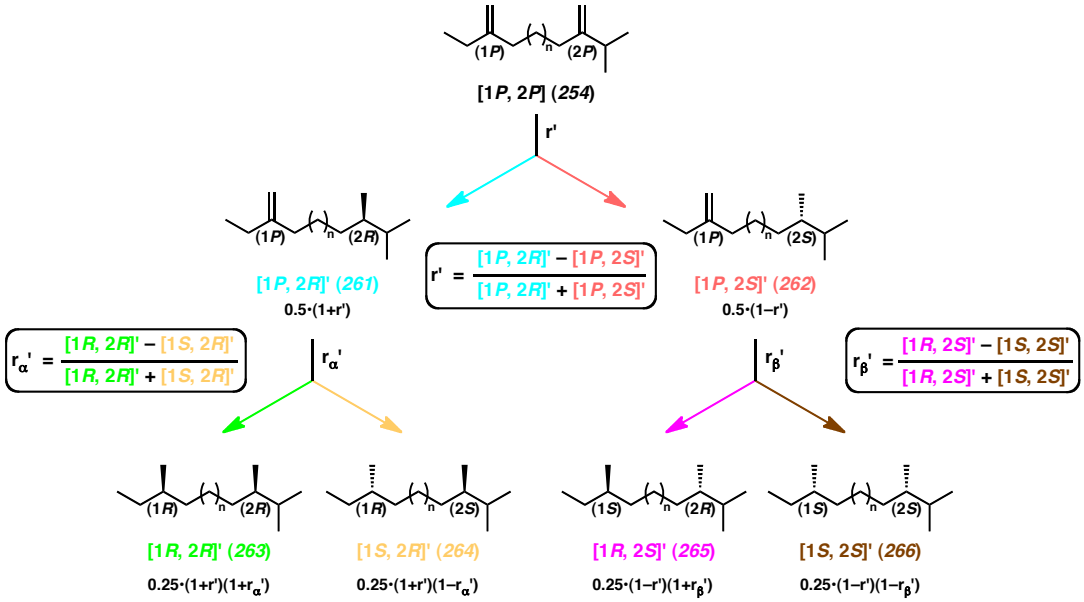

To be able to describe the course of a double asymmetric transformation as thoroughly as possible, another selectivity factor is required in addition to the six r type variables defined above. Because route 1 and route 2 both contribute competitively toward the final outcome of the reaction, the variable *i* must be established to determine the relative selectivity of the reaction for one route over the other. The *i* value is defined as the ratio between the quantity of material that reacts via route 1 and the total quantity of material that reacts via both routes 1 and 2. The *i* term is represented mathematically as follows:[16]

$$i = \frac{[1R, 2P] + [1S,2P]}{[1R, 2P] + [1S,2P] + [1P, 2R]' + [1P,2S]'} \quad (3)$$

A value of unity denotes complete selectivity for route 1, while a value of zero indicates complete selectivity toward route 2. An *i* value of 0.5 represents that equal portions of the starting material react along both available paths. With a total of seven selectivity variables defined, four stereoisomeric products to consider, and eight distinct

paths possible over the course of the reaction, a complete mathematical representation can be compiled. The relative contribution of each unique reaction pathway can be related to the values of dr, ee_A and ee_B.

$$ee_A = \frac{([1R, 2R] + [1R, 2R]') - ([1S, 2S] + [1S, 2S]')}{([1R, 2R] + [1R, 2R]') + ([1S, 2S] + [1S, 2S]')} = \frac{[i(1+r)(1+r_\alpha) + (1-i)(1+r')(1+r_\alpha')] - [i(1-r)(1-r_\beta) + (1-i)(1-r')(1-r_\beta')]}{[i(1+r)(1+r_\alpha) + (1-i)(1+r')(1+r_\alpha')] + [i(1-r)(1-r_\beta) + (1-i)(1-r')(1-r_\beta')]} \quad (4)$$

$$ee_B = \frac{([1R, 2S] + [1R, 2S]') - ([1S, 2R] + [1S, 2R]')}{([1R, 2S] + [1R, 2S]') + ([1S, 2R] + [1S, 2R]')} = \frac{[i(1+r)(1-r_\alpha) - (1-i)(1-r')(1+r_\beta')] - [i(1-r)(1+r_\beta) - (1-i)(1+r')(1-r_\alpha')]}{[i(1+r)(1-r_\alpha) - (1-i)(1-r')(1+r_\beta')] + [i(1-r)(1+r_\beta) - (1-i)(1+r')(1-r_\alpha')]} \quad (5)$$

$$dr = \frac{([1R, 2R] + [1R, 2R]') + ([1S, 2S] + [1S, 2S]')}{([1R, 2S] + [1R, 2S]') + ([1S, 2R] + [1S, 2R]')} = \frac{[i(1+r)(1+r_\alpha) + (1-i)(1+r')(1+r_\alpha')] + [i(1-r)(1-r_\beta) + (1-i)(1-r')(1-r_\beta')]}{[i(1+r)(1-r_\alpha) + (1-i)(1+r')(1-r_\alpha')] + [i(1-r)(1+r_\beta) - (1-i)(1-r')(1+r_\beta')]} \quad (6)$$

Equations (4), (5), and (6) are the most exhaustive mathematical representations of dr, ee_A, and ee_B available for any double asymmetric transformation. These complicated expressions allow for different selectivity values at every stage of the reaction, and thus account for every possible diastereomeric catalyst-substrate interaction. Because of this, these equations are ideal for situations where the influence of the substrate overpowers or complicates catalyst control.

In principle, manipulation of equations (4) through (6) should allow for examination of the various intermediate selectivity r values. Extracting these selectivity constants from observable data can provide insight into the total course of a double asymmetric transformation. Specifically, calculation of each r term could elucidate those phases of the reaction that operate with low or no selectivity. In light of this fact, attaining expressions for each individual r value could assist greatly in the optimization and understanding of these versatile processes. Unfortunately, while equations (4) through (6) do provide a maximum amount of theoretical information regarding every possible selectivity value, the number of variables employed in these expressions renders them intractable. With three equations, ten variables, and only three values readily attainable

from experimental observation, this most rigorous mathematic treatment is also impractical. In order to achieve a useful mathematical model, several simplifying assumptions must be made.

If the catalyst employed acts upon olefin (1) and olefin (2) with equal or reasonably similar efficacy, then each of the selectivity factors along route 2 can be assumed to be identical to the same r terms of route 1. In other words, each of the corresponding pairs of r values between the two routes can be taken as equal ($r = r'$, $r_\alpha = r_\alpha'$, and $r_\beta = r_\beta'$). Under this assumption, equations (4), (5), and (6), are reduced to the much more manageable expressions (7), (8), and (9). While these relationships are much less complicated than the alternatives presented above, they are nevertheless still difficult to engage realistically. The persistence of the *i* term in addition to the three r values, and the difficulty inherent in directly measuring any of these selectivity factors, once again provides a system of equations for which a solution is not attainable from the observable data.

$$ee_A = \frac{(1+r_\alpha)(1+r) - (1-r_\beta)(1-r)}{(1+r_\alpha)(1+r) + (1-r_\beta)(1-r)} \quad (7)$$

$$ee_B = (2i-1)\frac{(1-r_\alpha)(1+r) - (1+r_\beta)(1-r)}{(1-r_\alpha)(1+r) + (1+r_\beta)(1-r)} \quad (8)$$

$$dr = \frac{(1+r_\alpha)(1+r) + (1-r_\beta)(1-r)}{(1-r_\alpha)(1+r) + (1+r_\beta)(1-r)} \quad (9)$$

$i = 1$ ⇒

$$ee_A = \frac{(1+r_\alpha)(1+r) - (1-r_\beta)(1-r)}{(1+r_\alpha)(1+r) + (1-r_\beta)(1-r)} \quad (7)$$

$$ee_B = \frac{(1-r_\alpha)(1+r) - (1+r_\beta)(1-r)}{(1-r_\alpha)(1+r) + (1+r_\beta)(1-r)} \quad (10)$$

$$dr = \frac{(1+r_\alpha)(1+r) + (1-r_\beta)(1-r)}{(1-r_\alpha)(1+r) + (1+r_\beta)(1-r)} \quad (9)$$

⇒

$$r = \frac{dr \cdot ee_A + ee_B}{1 + dr} \quad (11)$$

$$r_\alpha = \frac{dr + dr \cdot ee_A - ee_B - 1}{dr + dr \cdot ee_A + ee_B + 1} \quad (12)$$

$$r_\beta = \frac{dr - dr \cdot ee_A + ee_B - 1}{dr \cdot ee_A - dr + ee_B - 1} \quad (13)$$

An important case to consider is the situation where the reaction displays total selectivity for either route 1 or route 2. Under these circumstances the value of *i* can be taken as 1, and the course of the reaction can be described fully via the use of only a single route (i.e., exclusively Scheme 3.10). This simplifies the situation to a system involving only the three selectivity factors (r, r_α, and r_β), and the three observable

stereoisomeric ratios (ee_A, ee_B, and dr). With the assumption of route exclusivity in place, equation (8) can be reduced to expression (10). Notably, the relationships described by (7), (9), and (10) can also be derived directly from the original expressions (4), (5), and (6) by assuming route selectivity ($i = 1$).

Further algebraic manipulation of equations (7), (9), and (10) provides access to expressions (11), (12), and (13), which describe the value of each selectivity factor in terms of the measurable quantities of ee_A, ee_B, and dr. Thus, under these limiting conditions the value of each intermediary selectivity variable can be evaluated and studied via directly observed experimental data. These mathematical representations therefore provide a method by which to scrutinize and optimize double asymmetric transformations by allowing the identification of mid-reaction processes with low or mediocre r values.

One further simplifying case that can be applied to equations (4)–(6) is a situation where the catalyst exerts a large influence on the reaction, but displays dissimilar selectivity values for transformation at either prochiral reactive site. In this system, it is assumed that two r variables representing the selectivity of reaction at either the 1P or 2P prochiral centers (r_1 and r_2, respectively) are sufficient to describe the course of a double asymmetric process (Scheme 3.12). The variable r_1 represents the selectivity of the transformation at the 1P center, regardless of the order in which the reactions occur. Whether considering the conversion of substrate **254** in route 1, or scrutinizing the reaction of intermediates **261** and **262** in route 2, every one of these processes is accepted to progress with a selectivity of r_1. The variable r_2 is defined similarly, and corresponds

to the selectivity of transformation at the 2P prochiral reactive site regardless of the route followed.

Scheme 3.12 Double asymmetric transformation via two variable simplification

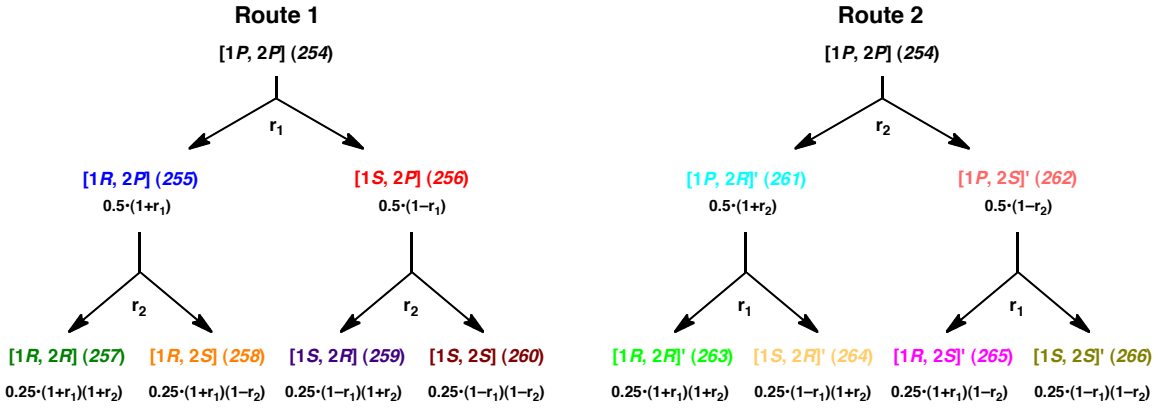

Using these relationships, it is possible to define expressions for ee_A, ee_B, and dr in terms of both the r_1 and r_2 variables. Examination of both routes 1 and 2 reveal that the final quantities of each stereoisomer afforded via either pathway are identical (i.e., [1R, 2S] = [1R, 2S]'). Because of this equivalence, the relationship between the selectivity variables and ee_A, ee_B, or dr are completely independent of the *i* term. This fact can be confirmed by using the quantities defined in Scheme 3.12 to calculate the three pertinent stereoisomeric ratios, thus attaining equations (14), (15), and (16), none of which display any dependence upon *i*. More importantly, these three expressions relate the measurable quantities of ee_A, ee_B, and dr to the value of r_1 and r_2, thereby reducing the system of multiple asymmetric transformations to a model involving only two unobservable variables. Notably, these same three equations may also be derived via direct substitution of the simplified r values ($r = r_1$, $r_\alpha = r_\beta = r_2$) into equations (4), (5), and (6).

$$ee_A = \frac{[i(1+r_1)(1+r_2) + (1-i)(1+r_1)(1+r_2)] - [i(1-r_1)(1-r_2) + (1-i)(1-r_1)(1-r_2)]}{[i(1+r_1)(1+r_2) + (1-i)(1+r_1)(1+r_2)] + [i(1-r_1)(1-r_2) + (1-i)(1-r_1)(1-r_2)]} = \frac{(1+r_1)(1+r_2) - (1-r_1)(1-r_2)}{(1+r_1)(1+r_2) + (1-r_1)(1-r_2)} = \boxed{\frac{r_1 + r_2}{1 + r_1 r_2}} \quad (14)$$

$$ee_B = \frac{[i(1+r_1)(1-r_2) + (1-i)(1+r_1)(1-r_2)] - [i(1-r_1)(1+r_2) + (1-i)(1-r_1)(1+r_2)]}{[i(1+r_1)(1-r_2) + (1-i)(1+r_1)(1-r_2)] + [i(1-r_1)(1+r_2) + (1-i)(1-r_1)(1+r_2)]} = \frac{(1+r_1)(1-r_2) - (1-r_1)(1+r_2)}{(1+r_1)(1-r_2) + (1-r_1)(1+r_2)} = \boxed{\frac{r_1 - r_2}{1 - r_1 r_2}} \quad (15)$$

$$dr = \frac{[i(1+r_1)(1+r_2) + (1-i)(1+r_1)(1+r_2)] + [i(1-r_1)(1-r_2) + (1-i)(1-r_1)(1-r_2)]}{[i(1+r_1)(1-r_2) + (1-i)(1+r_1)(1-r_2)] + [i(1-r_1)(1+r_2) + (1-i)(1-r_1)(1+r_2)]} = \frac{(1+r_1)(1+r_2) + (1-r_1)(1-r_2)}{(1+r_1)(1-r_2) + (1-r_1)(1+r_2)} = \boxed{\frac{1 + r_1 r_2}{1 - r_1 r_2}} \quad (16)$$

The most extreme limiting case to consider for equations (4)–(6) is the situation in which the catalyst employed exercises complete and identical control over all stages of enantioselective bond construction. Such an assumption would be reasonable for substrates where both of the reactive sites are considerably removed from one another and are similarly reactive. Under these circumstances, all selectivity values can be taken as equal ($r = r_\alpha = r_\beta = r' = r_\alpha' = r_\beta'$). If route selectivity is once again considered exclusive ($i = 1$), then equations (4)–(6) are easily reduced to two simple expressions, with the value of ee_B being equal to zero in all cases.

$$\boxed{ee_A = \frac{2r}{1 + r^2}} \quad (17) \qquad ee_B = 0 \quad (18) \qquad \boxed{dr = \frac{1 + r^2}{1 - r^2}} \quad (19)$$

Equations (17) and (19) closely resemble the mathematical representation of the Horeau principle described by expressions (1) and (2), with the selectivity factor r taking the place of the monomer enantiomeric excess (ee_i). Because these relationships represent an extremely aggressive reduction of equations (4), (5), and (6), their application should only be appealed to after careful consideration of the simplifying assumptions in use. Specifically, great confidence must be placed in the ability of the catalyst to operate upon all prochiral sites with equal efficacy and selectivity.

The relationship between the selectivity factors employed in the equations above and the final values of ee_A, ee_B, and dr are not immediately obvious from their mathematical

representations. In order to better depict the influence of the r values upon the stereoisomeric ratios of the products, the simplified expressions presented in equations (14), (15), and (16) can be represented graphically.

Because the value of ee_A and dr are most often of interest in double asymmetric transformations, their relationship to values r_1 and r_2 are represented below (Figure 3.2, 3.3). Examination of these three-dimensional plots reveals a striking similarity to the plotted behavior of the ee_f and *de* values for the expressions of the Horeau duplication (Figure 3.1). Plotting equation (16) illustrates the diastereomeric enrichment of the reaction product as it relates to either selectivity factor, and from this graph one can observe a negative non-linear deviation in *de* relative to both r values (Figure 3.2A).[19] Indeed, in these cases, the ultimate *de* of the reaction product is always less than either of the selectivity factors alone. As either r_1 or r_2 approaches zero, the product *de* drops precipitously, and does so regardless of the remaining r value. Because of this, only in situations where both r_1 and r_2 are simultaneously large will the dr of the reaction be reasonably high.

Investigation of the behavior of ee_A as it relates to the r_1 and r_2 selectivity terms (i.e., plotting equation (14) in three dimensions) reveals a relationship similar to the positive non-linear deviations calculated for Horeau-type duplications. In fact, if a substitution is made where both r terms are equal, this relationship reduces exactly to the Horeau-type model (i.e., setting $r_1 = r_2$ in expression (14) will afford the ee_f graph of Figure 3.1). The graph depicted in Figure 3.2B illustrates the impact of both selectivity values upon the overall enantioenrichment of the major diastereomer in a double asymmetric process. This plot clearly demonstrates that the value of ee_A rises rapidly in response to any

increase in either r_1 or r_2 alone. Scrutiny of both the graphical and mathematical representations of ee_A clearly demonstrates that the lower bound for this term is defined by the highest r value in operation. Indeed, when both r terms are nonzero values, the final value of ee_A will always exceed both of the independent selectivity factors, and thus rapidly approach unity.[20]

Figure 3.2 Product (A) ee_A*, (B)* de*, and (C) both plotted as a function of* r_1 *and* r_2 *selectivity factors*

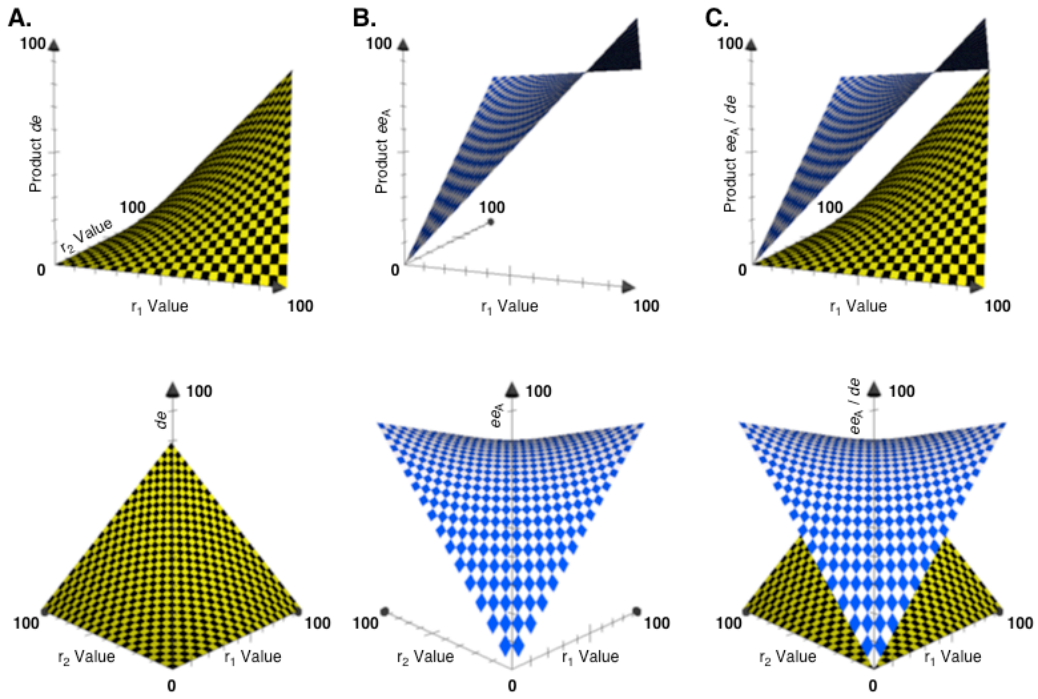

The graphs in this figure include: (A) Three-dimensional plot of an adaptation of equation (16), relating r_1 and r_2 to final product *de*, (B) Three-dimensional plot of equation (14), relating r_1 and r_2 to final product ee_A, and (C) Simultaneous three-dimensional plot of both equations (14) and (16). All values are presented in terms of percentage.

By simultaneously plotting the surfaces representing ee_A and *de* as they relate to any value of r_1 and r_2, the costs and benefits of multiple asymmetric transformation are clearly displayed (Figure 3.2C). Exceptions levels of enantioenrichment in the major diastereomer can be attained with even modest selectivity, but the corresponding values

of *de* increase much more slowly. Just as in the case of Horeau duplication, high product enantioselectivity is attained in a multiple asymmetric transformation at the cost of yield sacrificed to the minor diastereomer.[21]

To better illustrate the interplay between the r terms and the values of ee_A and dr, it is useful to consider the case wherein one enantioselective process occurs with total selectivity, and the other occurs with none whatsoever (Scheme 3.13). If the initial bond-forming reaction establishes the new stereocenter with an r value of 1, then the prochiral starting material [1P, 2P] (**254**) will be exclusively converted into intermediate [1R, 2P] (**255**). Regardless of the selectivity encountered in the subsequent reaction, because no possibility exists for the formation of the [1S, 2S] isomer, ee_A will always be 100%. However, because it is assumed that the subsequent transformation occurs with no preference for either diastereomer, both [1R, 2R] (**257**) and [1R, 2S] (**258**) isomers are produced in equal quantities, yielding a dr of 1 : 1 for the final product.

Scheme 3.13 Double asymmetric transformation where $r_1 = 1.0$ and $r_2 = 0$

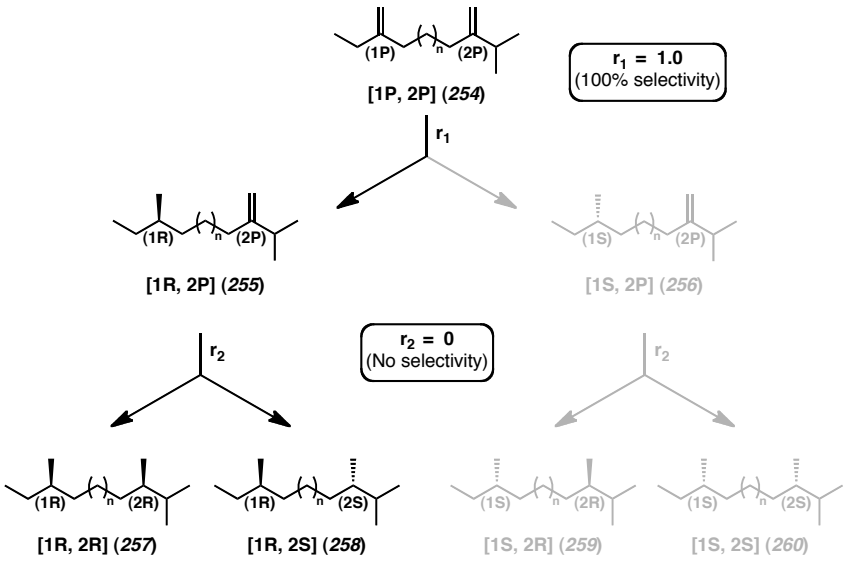

In the situation where the initial bond-forming reaction occurs with no selectivity ($r_1 = 0$), equal portions of [1R, 2P] (**255**) and [1S, 2P] (**256**) are afforded (Scheme 3.14). However, in this theoretical case it is assumed that both intermediates subsequently undergo an asymmetric reaction that occurs with total selectivity ($r_2 = 1$). Therefore, stereoisomers [1R, 2R] (**257**) and [1S, 2R] (**259**) are produced as the sole products of reaction, and in equal quantities. Again, while the final dr value resulting from this transformation is 1 : 1, the ultimate ee_A is 100%. Just as in the case of the Horeau-type duplications, the positive amplification observed in product *ee* can be attributed to the creation and removal of an undesired diastereomeric product. Thus, even in the case of multiple asymmetric transformations, increased *ee* comes at the cost of decreased dr and sacrificed yield. Also, whereas ee_A shows a dependence upon only one of the r terms in operation, the value of dr relies heavily upon both r_1 and r_2 together.

Scheme 3.14 Double asymmetric transformation where $r_1 = 0.0$, and $r_2 = 1.0$

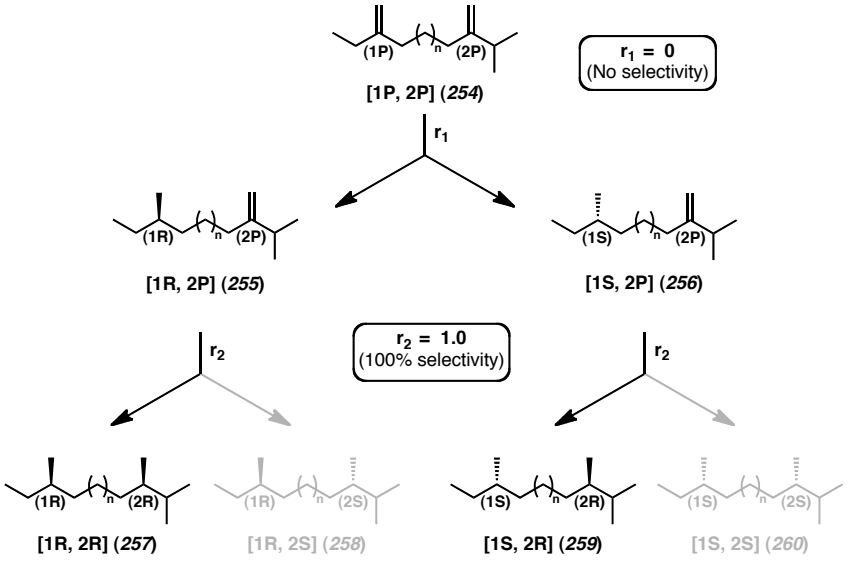

Further examples of the interplay between r_1 and r_2 with the value of ee_A and dr are summarized in Table 3.2 below. Notably, these theoretical cases illustrate the relative insensitivity of the ee_A term with regard to either selectivity value, and the much greater dependence of dr upon r_1 and r_2 simultaneously. Indeed, only when both selectivity terms achieve a value of 95% does the dr reach a level of 20 : 1, a number typically regarded as being excellent.

Table 3.2 Selected examples of r_1 and r_2 values, and their impact on ee *and* de

r_1 (%)	r_2 (%)	ee_A (%)	de (%)	dr	yield lost (%)
0	100	100	0	1 : 1	50
100	0	100	0	1 : 1	50
50	50	80	25	1.7 : 1	38
50	75	91	38	2.2 : 1	31
50	90	96	45	2.6 : 1	28
75	90	98	68	5.2 : 1	16
90	90	99	81	9.5 : 1	10
95	95	>99	90	20 : 1	5

It is important to note that the equations presented above cover a wide range of possible circumstances, and that care must be taken to apply the most appropriate formulae for a given reaction. While equations (17) and (19) are undeniably the most mathematically accessible expressions, these expressions should only be employed in situations where the degree of catalyst control is exceptionally high. These simplified expressions can also be applied when both of the prochiral reactive sites are very similar in terms of reactivity, and are also sufficiently distal from one another, so as to preclude intramolecular interference. For circumstances where catalyst control is anticipated to be high, but nevertheless operate with dissimilar selectivity at different prochiral reactive sites, equations (14)–(16) should be used. In those situations where catalyst control is not

absolute, but the order of transformation is limited to a single route exclusively, equations (11)–(13) should be used to investigate the three distinct selectivity values involved. Under conditions where substrate-catalyst interactions are likely to have a significant influence upon selectivity at all stages of bond construction, the rigorous equations (4)–(6) must be employed.

3.2.5 SYNTHETIC APPLICATIONS OF MULTIPLE ASYMMETRIC TRANSFORMATIONS

Multiple asymmetric transformations have proven to be a powerful and efficient technique when employed in the context of natural products total synthesis. Several groups have reported the use of highly selective catalysts for the rapid, simultaneous construction of key bonds in critical synthetic intermediates. These powerful, concurrent bond-forming processes have facilitated the preparation of complicated molecules with a minimal investment of time and effort.[22,23,24]

One impressive example of a practical double asymmetric transformation in total synthesis can be found in Overman's approach toward quadrigemine C.[25] Starting with dibutenanilide **267**, treatment with palladium acetate and (*R*)-Tol-BINAP initiated two simultaneous, stereocontrolled Heck reactions (Scheme 3.15). The eventual product of this transformation was dioxindole **268**, which was isolated in 90% *ee* and as a 3 : 1 ratio with the undesired *meso* diastereomer. The rapid construction of two all-carbon quaternary stereocenters in high enantiopurity made the completion of the total synthesis possible in only two additional steps. In this situation, it is notable that nearly 20% of the dibutenanilide **267** was lost to the *meso* diastereomer generated in the course of reaction,

once again illustrating the costs inherent to multiple asymmetric transformations. Nevertheless, both the speed and selectivity with which Overman is able to conclude the total synthesis of quadrigemine C (**269**) justify this sacrifice.

Scheme 3.15 Double asymmetric catalytic transformation toward quadrigemine C

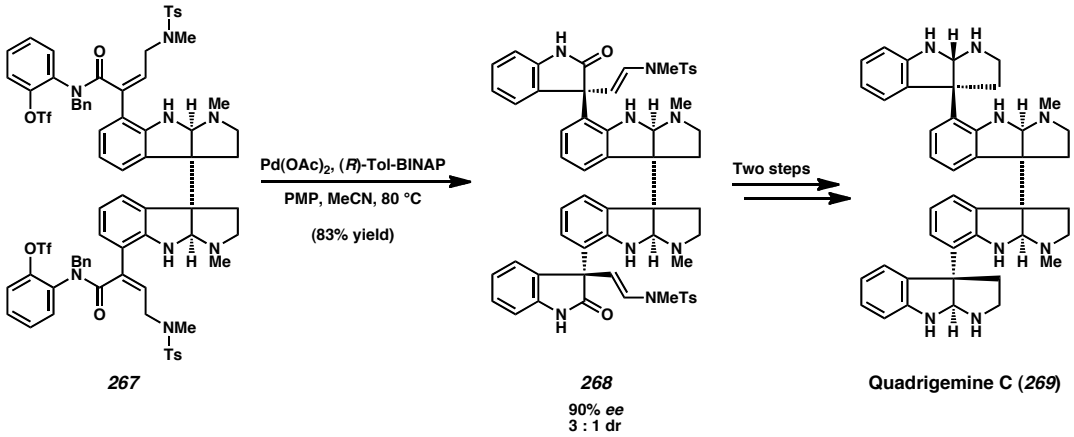

The drawbacks of multiple asymmetric transformations can be overcome under circumstances where the catalyst employed exerts a high degree of control at all stages of bond construction. An impressive example of catalyst preference overriding substrate interference across multiple bond-forming events can be found in the total synthesis of glabrescol (**273**) performed by Corey and coworkers (Scheme 3.16).[26] Exposure of tetraol **270** to Shi's chiral dioxirane conditions[27] smoothly afforded tetraepoxide product **272** in 66% yield and an estimated 80% diastereomeric purity. In light of the fact that four asymmetric processes must occur to form all eight of the new stereocenters found in tetraol **272**, each epoxidation step in this reaction must have transpired with greater than 20 : 1 selectivity (r = 90%) in order to attain the experimentally observed level of diastereoselection. Given the number of distinct diastereomeric intermediates possible throughout the course of this reaction, as well as the potential for deleterious catalyst-

substrate interactions to deteriorate the desired selectivity, the ability of the Shi catalyst to exert this level of control is impressive. By leveraging this powerfully selective technique, Corey was able to set eight of the ten stereocenters of glabrescol in a single, efficient procedure. Conclusion of the synthesis was thereafter attained in only three additional steps.

Scheme 3.16 Total synthesis of glabrescol by Corey

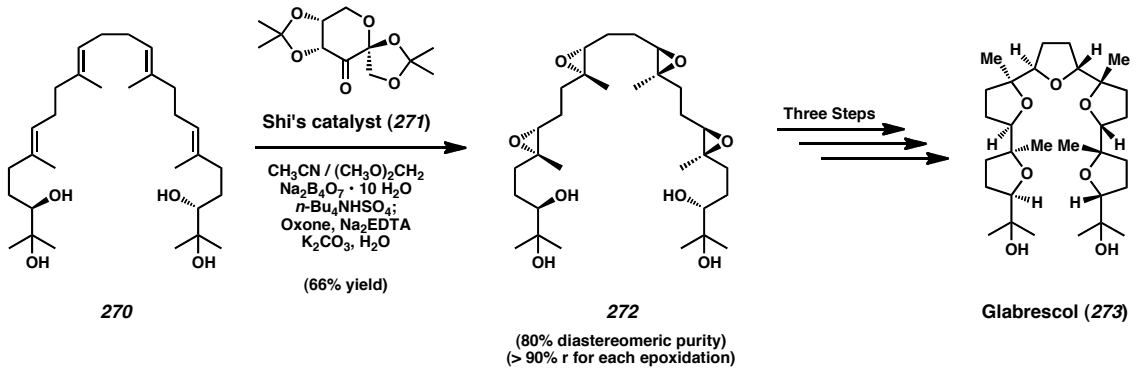

The same approach that Corey proved to be effective toward the total synthesis of glabrescol was later applied toward the preparation of the oxasqualenoid natural product omaezakianol (**276**, Scheme 3.17).[28] Starting from pentaolefin substrate **274**, use of the Shi catalyst to generate enantioenriched pentaepoxide **275** was followed by treatment under acidic conditions and subsequent exposure to sodium metal. This three-step process afforded access to omaezakianol (**276**) in 16% yield as a single, enantiopure diastereomer. The efficiency of this synthetic sequence, as well as the stereopurity of its eventual product, would not be possible without the application of a refined multiple asymmetric transformation.

Scheme 3.17 Total synthesis of omaezakianol by Corey

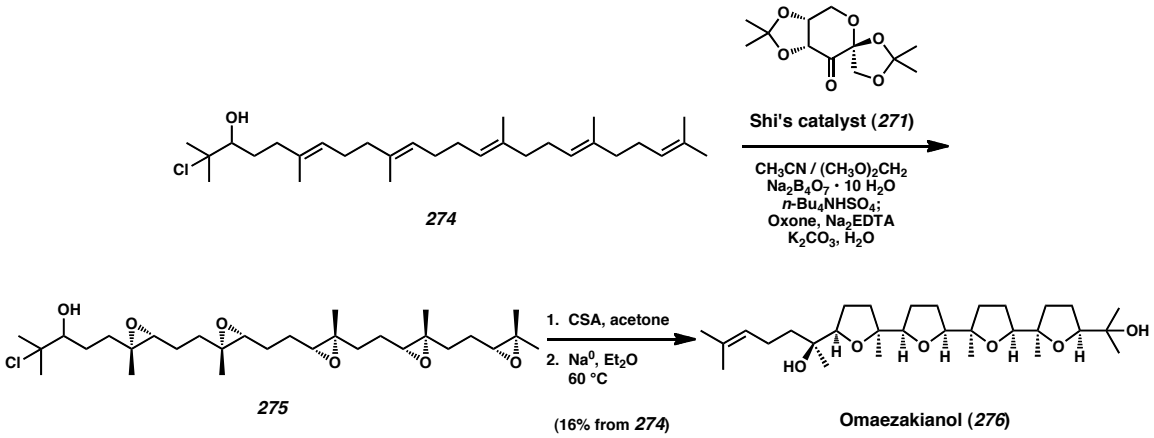

3.3 EXPERIMENTAL INVESTIGATION OF MULTIPLE ASYMMETRIC TRANSFORMATIONS

After having scrutinized the literature for a thorough mathematical explanation of multiple asymmetric transformations and Horeau duplications, we turned our focus once more toward the case of our double asymmetric catalytic alkylation reactions (Schemes 3.18A, 3.18B). With equations (17) and (18) in mind, we reasoned that the lower than desired diastereomeric ratio obtained in the generation of diketone **185** and cyclohexanone **224** must be the result of a less than optimal r_1 or r_2 value. A mediocre selectivity operating at one or both of the alkylation steps in these reactions could be responsible for lower than anticipated dr values observed, while still providing exceptional enantiopurity in the desired products.

Scheme 3.18 Examples of double asymmetric catalytic alkylation

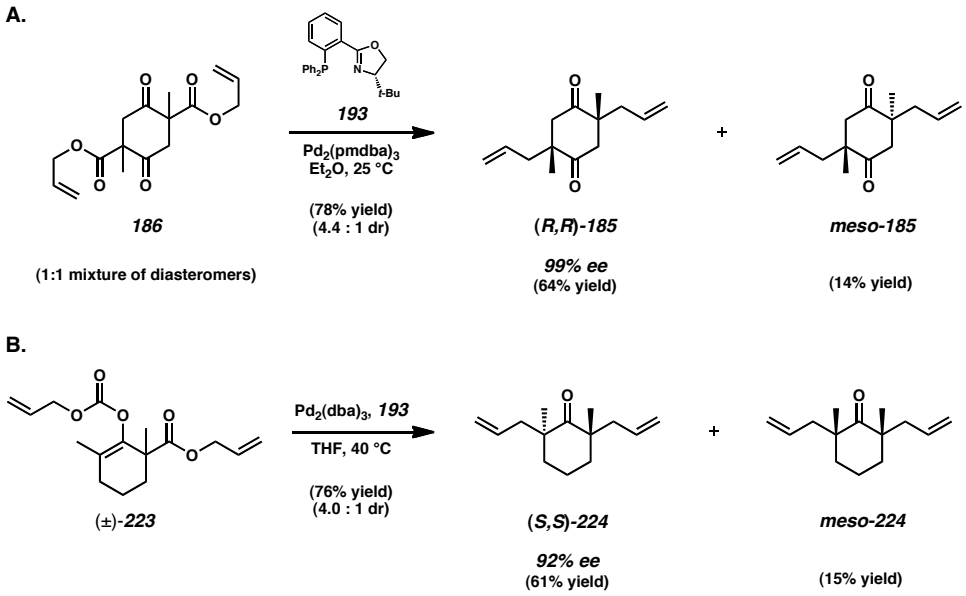

In order to optimize our results to achieve higher dr values, we hoped to use data extracted from the mathematical relationships described in the preceding sections to determine at which point in the reaction process the selectivity was less than desired. Unfortunately, due to the symmetric and achiral nature of the minor *meso* diastereomer in these reactions, it is not possible to collect data concerning ee_B in either of these reactions. Because of this fact, we were unable to implement equations (4)–(6), (11)–(13), or (14)–(16) to obtain data concerning the selectivity of the primary or secondary bond-forming events. Instead, we appealed to limiting cases of expressions (17) and (19) to gain insight into the possible range of values that either r term might possess. For example, if a value of 80% were in operation for both r_1 and r_2 variables, this would result in an ee_A of 98%, and a dr of 4.5 : 1. Additionally, if the r_1 and r_2 selectivities had dissimilar values of 95% and 65%, respectively, this would result in an ee_A of 99%, and a dr of 4.2 : 1. Both sets of possible r values are reasonably close to the experimentally observed results for both transformations. However, in the absence of a measurable ee_B

value, a clear understanding of the selectivities in operation cannot be calculated with confidence.

An additional point of complication involved with the double alkylation of either bis(β-ketoester) **186** (Scheme 3.18A) or enol carbonate (±)-**223** (Scheme 3.18B) is the presence of a pre-existing stereocenter during both asymmetric transformations. Initial decarboxylation of either of these substrates will lead to reactive ketone enolate intermediate bearing a "spectator" stereocenter (**277** or **279**).[29] During the first enantioselective bond formation, either intermediate **227** or **279** will be present in solution as a racemic mixture.

*Scheme 3.19 Schematic representation of intermediates in the double asymmetric alkylation of (A) substrate **186**, and (B) substrate (±)-**223***

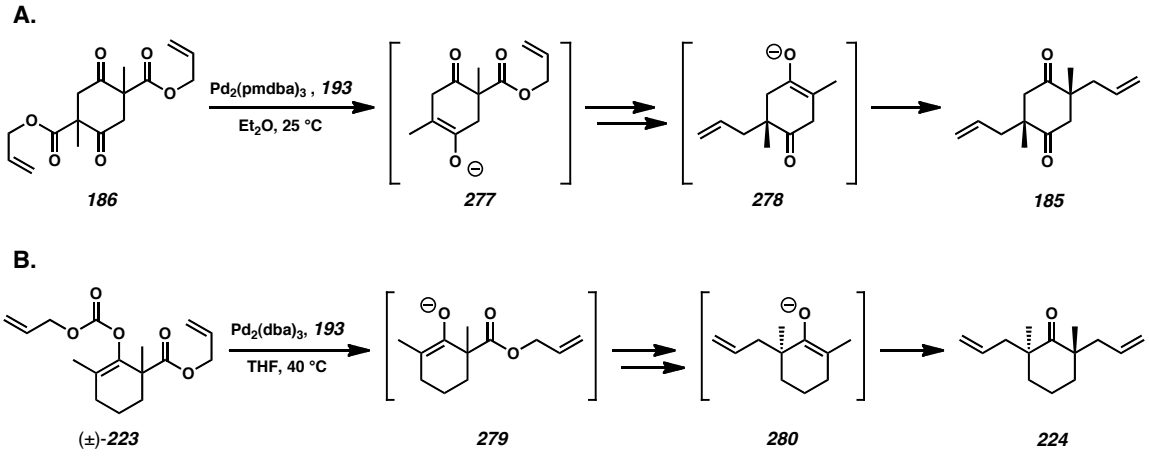

After alkylation of the transient enolate and subsequent decarboxylation of the remaining β-ketoester, the resulting enolate intermediates **278** and **280** still possess a "spectator" stereocenter. However, unlike the previous alkylation process, at this point in the reaction anionic intermediates **278** and **280** are enantioenriched to some extent by the action of the previously selective bond formation. Because the primary alkylation acts

upon a racemic mixture, whereas the secondary alkylation engages an enantioenriched substrate, the corresponding r values for each step are anticipated to be dissimilar due to their different stereochemical features. In order to better understand the impact of pre-existing stereocenters upon a double asymmetric transformation, we decided to first investigate the stereoselective alkylation of a racemic substrate. Toward this end, we synthesized enol carbonate (±)-**281**, and subjected this material to the conditions of asymmetric alkylation to afford a mixture of racemic cyclohexanone diastereomers (**282**, Scheme 3.19A).

*Scheme 3.20 (A) Alkylation of racemic enol carbonate (±)-**281** and (B) mathematical treatment thereof*

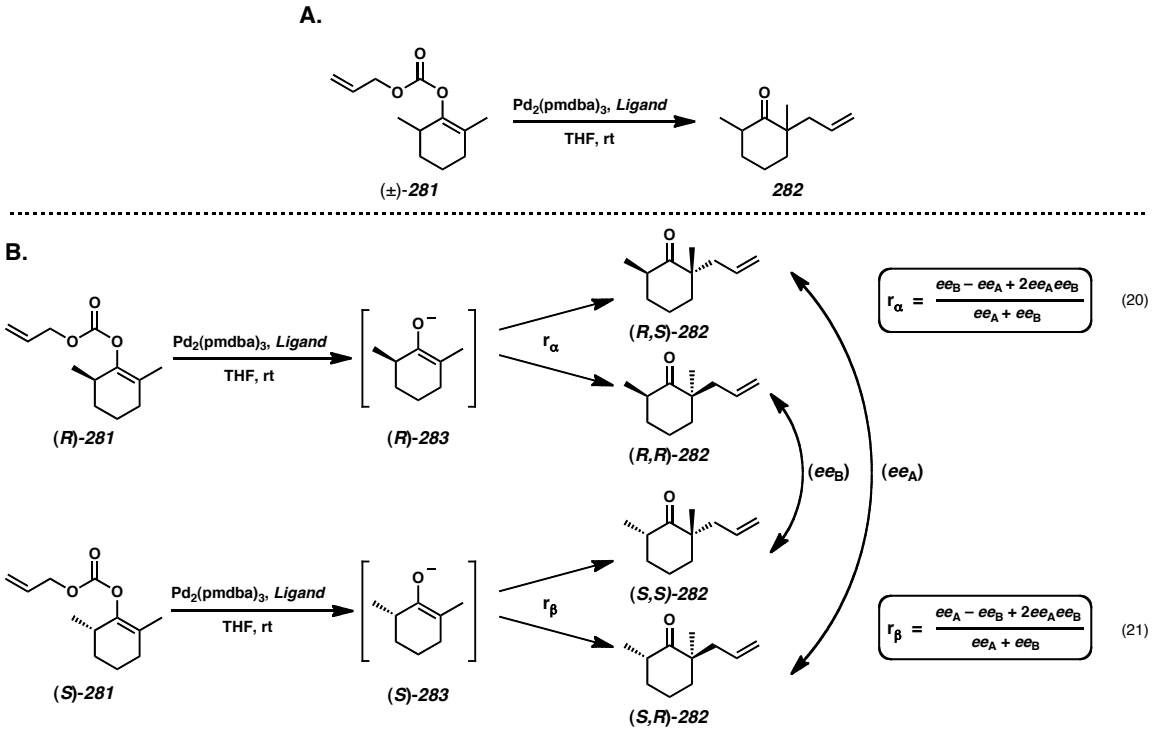

Starting from the racemic enol carbonate (±)-**281**, it is possible to represent the possible stereochemical pathways of the reaction mathematically (Scheme 3.19B). As a

racemate, carbonate (±)-**281** must enter the reaction as a 1 : 1 mixture of enol enantiomers (*R*)-**281** and (*S*)-**281**. Upon initiation of the reaction, both of these stereoisomers undergo decarboxylation to afford an enantiomeric pair of ketone enolate intermediates ((*R*)-**283** and (*S*)-**283**). Interaction of these intermediates with an enantioenriched catalyst thereafter generates a pair of diastereomeric catalyst-substrate complexes, both of which undergo the alkylation process with a distinct selectivity value (r_α and r_β, as defined in Scheme 3.19B). By analyzing the magnitude of ee_A and ee_B, as well as both the r_α and r_β values, information about the interplay between catalyst and substrate can be extracted from experimental data. Interestingly, the mathematical representation of this reaction can be considered a special case of equations (7), (9), and (10), wherein the selectivity for the primary alkylation is taken to be zero (r = 0). This affords expressions for ee_A, ee_B, and dr that rely exclusively upon the r_α and r_β terms. Algebraic manipulation of these formulae yields expressions (20) and (21), relationships that allow for the calculation of either selectivity factor from observable *ee* data.

Under conditions involving a high degree of catalyst control, it would be expected that the values of both r_α and r_β would approach unity, in accordance with ligand-guided bond construction. In such a situation, the reaction would afford a 1 : 1 mixture of enantiopure diastereomers ((*R*,*S*)-**282** and (*S*,*S*)-**282**, exclusively). However, the possibility exists that alkylation of enolates (*R*)-**283** and (*S*)-**283**) may operate with an overwhelming substrate preference for a particular relative stereochemical configuration (favoring either (*R*,*S*)-**282** and (*S*,*R*)-**282**, or (*R*,*R*)-**282** and (*S*,*S*)-**282**). In this case, the substrate interference would overpower catalyst selectivity to yield a very large dr, as well as one r term much larger than the other ($r_\alpha > r_\beta$, or $r_\alpha < r_\beta$). This would result in one

matched, and one mismatched, catalyst-substrate interaction. Such a process would be expected to generate exceptionally high levels of dr, but afford minimal values for either *ee*.

Subjecting enol carbonate (±)-**281** to the conditions of the enantioselective alkylation allowed us to gain some insight into the behavior of this reaction in the presence of pre-existing stereocenters. Substrate (±)-**281** was alkylated in the presence of numerous different ligands, a small subset of which results are summarized below (Table 3.3).

Table 3.3 Study on the effect of a pre-existing stereocenter upon asymmetric alkylation[a]

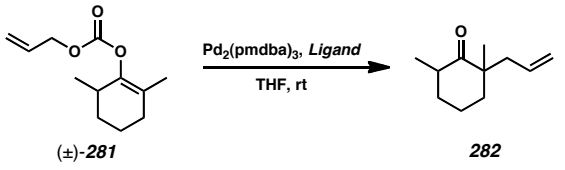

(±)-***281*** ***282***

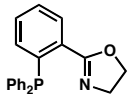

284

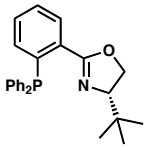

193

Ligand	Yield (%)	dr	ee_1	ee_2	r_α	r_β
PPh_3	49%	4.5:1	-	-	64%	–64%
284	79%	24:1	-	-	92%	–92%
193	81%	2.7:1	40%	99%	99%	10%
285	48%	2.2:1	36%	79%	87%	12%
286	-	15:1	5.9%	78%	97%	–78%

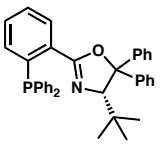

285

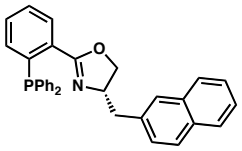

286

[a] All values presented were measured from collected GC data, rather than expressions (20) or (21).

Based on the data collected from these experiments, the r_α value appears to be large across most cases. Regardless of the ligand employed, the ratio of alkylation for intermediate (*R*)-**283** appears to strongly favor (*R*,*R*)-**282** over (*R*,*S*)-**282**, suggesting a matched catalyst-substrate situation. Conversely, the r_β value was observed to be disappointingly low for many of these experiments, often favoring the formation of stereoisomer (*S*,*R*)-**282** against catalyst preference. This trend in r_β suggests that the substrate interferes directly and considerably with the catalyst system over the course of

the enantioselective bond-forming event. In order to further evaluate these findings, the alkylation of an enantioenriched substrate bearing a pre-existing stereocenter was examined.

To more thoroughly study the impact of pre-existing stereocenters upon the course of a double asymmetric alkylation reaction, the enantiopure β-ketoester **287** was prepared as a mixture of diastereomers (Scheme 3.20). Exposure of **287** to the previously described allylation conditions afforded cyclohexanone **224** in greater than 50 : 1 dr (C_2 : *meso*). This diastereomeric ratio indicates that the selectivity of alkylation on **287** proceeds with an r value of approximately 96%.[30] Repeating this experiment with (*R*)-*t*-BuPHOX instead of (*S*)-*t*-BuPHOX provided cyclohexanone **224** in a 1 : 6.7 dr (C_2 : *meso*). If this diastereomeric ratio is converted to an alkylation selectivity value, an r term equal to –74% is obtained.[31] Though this reversal of selectivity indicates some measure of catalyst control during bond formation, the reduced magnitude of the diastereomeric ratio reveals that catalyst preference is not operating uncontested.

Scheme 3.21 Asymmetric alkylation of an enantioenriched substrate[a]

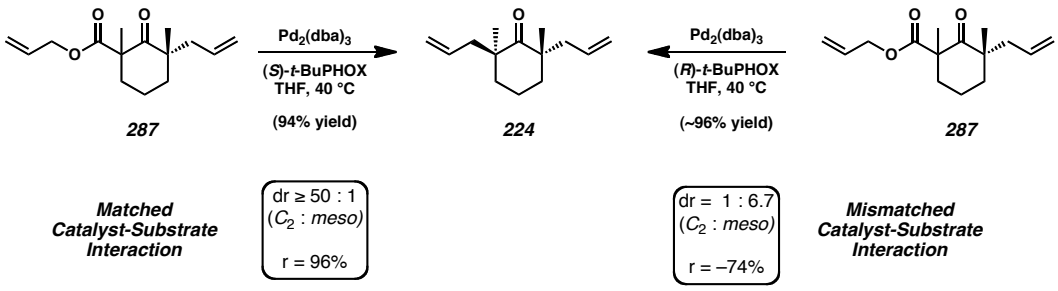

[a] For the reaction involving (*S*)-*t*-BuPHOX, use of either isolated, pure diastereomer of β-ketoeseter ***287*** afforded cyclohexanone ***224*** in excess of 50 : 1 dr. Additionally, a 1 : 1 mixture of both possible diastereomers of ***287*** achieved the same result. For the reaction involving (*R*)-*t*-BuPHOX, use of a pure diastereomer of ***287*** or a 1 : 1 mixture of diastereomers gave cyclohexanone **224** in a 1 : 6.7 dr. Relative stereochemistry of the isomers of ***287*** was not assigned.

Overall, the exceptionally high dr observed with the use of (*S*)-*t*-BuPHOX and β-ketoester **287** strongly suggests a matched catalyst-substrate situation, whereas the lower selectivity observed when (*R*)-*t*-BuPHOX is employed indicates some degree of mismatched interference. With these findings in mind, it is likely that the development of deleterious catalyst-substrate interactions due to the presence of pre-existing stereocenters, in combination with negative non-linear (Horeau-type) statistical effects, are the factors responsible for the lower than anticipated diastereomeric ratio values observed in our double-alkylation experiments. However, given the exceptional level of diastereoselectivity observed in these reactions when (*S*)-*t*-BuPHOX is employed, the results strongly suggest that undesired interactions influence the initial alkylation process, rather than the secondary allylation. If the allylation of enolate **279** (Scheme 3.19) in the double asymmetric alkylation were to proceed with high catalyst selectivity, the reaction would necessarily intercept an intermediate similar to β-ketoester **287** in the course to the final reaction product. In keeping with the results presented above, an exceptional dr would be anticipated under these conditions. Because the double asymmetric alkylation of (±)-**223** was observed to afford a 4.0 : 1 value for dr, these experiments suggest that the primary allylation occurs with mediocre selectivity.

To further strengthen our understanding of double asymmetric alkylation processes, additional investigations were performed using the racemic enol carbonates (±)-**288** and (±)-**290** (Scheme 3.21). Though very similar to the previously discussed enol carbonate (±)-**223**, these modified substrates possess differential substitution on either side of the latent ketone functionality. This critical addition provides two analytical advantages over the more symmetric ester (±)-**223**. First, due to the structural nature of these

differentially substituted, masked β-ketoester compounds, it is possible to control the order in which the alkylation events occur, thus restricting the course of the reaction to a single route (i = 1). Second, double alkylation of either (±)-**288** or (±)-**290** yields cyclohexanone **289** as the terminal product, allowing for direct comparison of results between the two orders of alkylation. Lastly, when considering the four stereoisomers of cyclohexanone **289** that can be afforded by these reactions, none of the possible diastereomers predicted are *meso* in nature, thus allowing for direct observation of ee_B. Because of this, more complicated mathematical expressions can be applied to the system in order to extract selectivity data, rather than relying upon the oversimplified equations (17) and (19).

Scheme 3.22 Substrates for double asymmetric catalytic alkylation studies

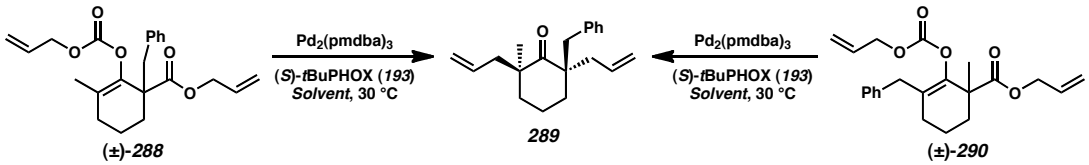

Both esters (±)-**288** and (±)-**290** were exposed to a palladium(0) precatalyst and (*S*)-*t*-BuPHOX (**193**) across twelve solvents at two concentrations (Scheme 3.22). The results of these reactions were scrutinized for the critical values of ee_A, ee_B, and diastereomeric ratio.[32] Because the β-ketoester moiety nested in both substrates (±)-**288** and (±)-**290** is effectively masked, reaction of either molecule can be assumed to first occur from the enol carbonate functionality. This reduces the possible number of selectivity factors encountered to three, thus allowing equations (11) – (13) to be implemented when calculating the value of these r terms. It is critical to note that equations (11) – (13)

facilitate more complicated calculations, provide more detailed data, and involve fewer simplifying assumptions than expressions (14)–(16), because of their inclusion of an additional r term. As such, the following case is no way comparable to the graphs presented in Figure 3.2.

Scheme 3.23 Stereochemical course of double alkylation for a differentially substituted carbonate

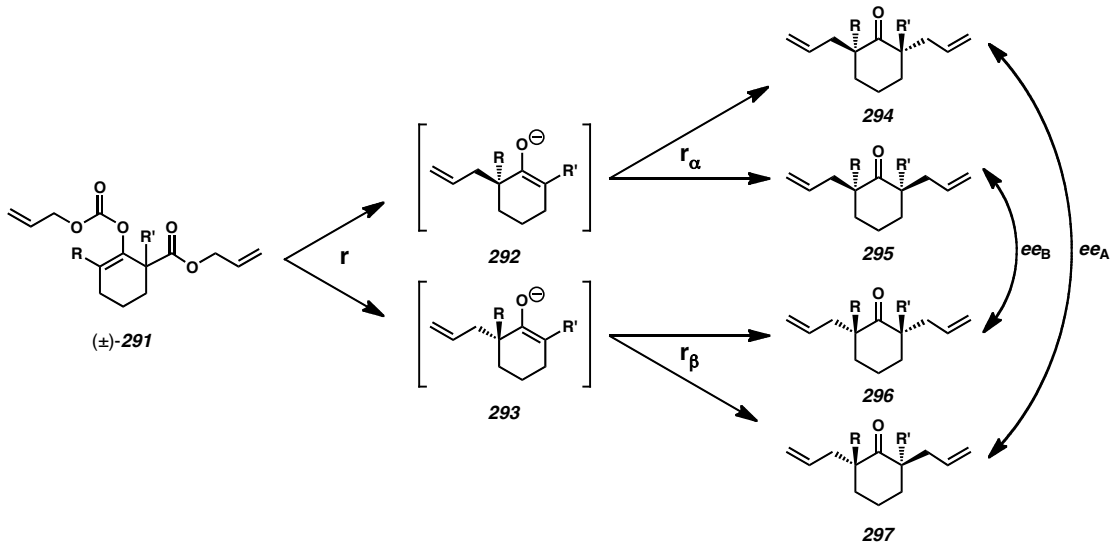

$$r = \frac{292 - 293}{292 + 293} = \frac{dr \cdot ee_A + ee_B}{1 + dr} \quad (11)$$

$$r_\alpha = \frac{294 - 295}{294 + 295} = \frac{dr + dr \cdot ee_A - ee_B - 1}{dr + dr \cdot ee_A + ee_B + 1} \quad (12)$$

$$r_\beta = \frac{296 - 297}{296 + 297} = \frac{dr - dr \cdot ee_A + ee_B - 1}{dr \cdot ee_A - dr + ee_B - 1} \quad (13)$$

Examination of the data resulting from these reactions provided surprising insight into the course of the double asymmetric catalytic alkylation (Scheme 3.24). Nearly every reaction run displayed a large value of ee_A, typically between 85 and 90 percent. The value of ee_B in all cases was only slightly lower, averaging between 75 and 85 percent. Across all experiments performed, the diastereomeric ratio observed ranged from 1.5 : 1 to 6.2 : 1, with the vast majority of results between 2.5 : 1 and 3.5 : 1. These

data are consistent with literature precedent regarding the positive non-linear effects anticipated for the value of ee_A and the negative non-linear effects anticipated for dr.

Scheme 3.24 Averaged selectivity values for double asymmetric catalytic alkylation

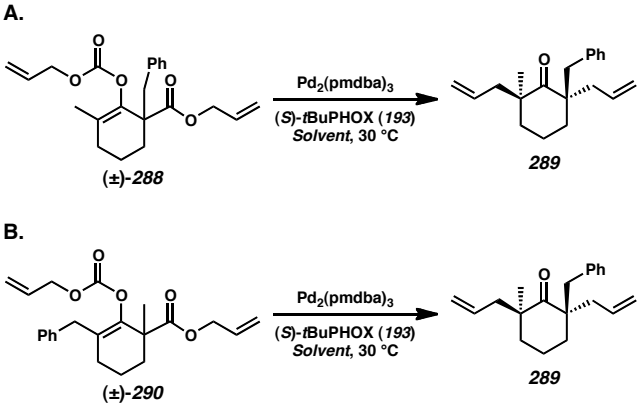

Average Values							
[0.03 M]				[0.01 M]			
ee_A	89.1%	r	87.1%	ee_A	90.6%	r	89.2%
ee_B	81.2%	r_α	42.8%	ee_B	84.6%	r_α	42.6%
dr	2.5:1	r_β	–14.8%	dr	2.6:1	r_β	–10.2%

Average Values							
[0.03 M]				[0.01 M]			
ee_A	83.0%	r	82.6%	ee_A	85.1%	r	84.5%
ee_B	78.8%	r_α	56.6%	ee_B	80.6%	r_α	56.0%
dr	3.9:1	r_β	–45.0%	dr	3.8:1	r_β	–39.6%

Using the data obtained from these experiments in combination with the equations discussed previously, values for all three selectivity terms can be derived. In all reactions examined the value of the r term averages above 80%, and typically falls within the range between 85 and 90%. This finding implies two important facts about the course of the double alkylation reaction. First, these data indicate that the initial bond-forming event proceeds with the close to the expected degree of catalyst control. Second, because the value of r is large, the total quantity of intermediate enolate **293** present throughout the reaction is very small (Scheme 3.23). It should be noted that a majority of the calculated r_β values afford negative results, indicating a preference for the generation of cyclohexanone **297** over diallyl species **296** during the final bond-forming transformation. However, due to the sparingly small quantity of enolate **293** produced from the previous alkylation, the influence of r_β upon the overall outcome of the reaction

is minimized. As such, no trend is easily observable between the value of r_β and either ee_A or dr.

In light of the consistently large selectivity for r, and the consequent insignificance of r_β, the r_α term appears to be much more important to the eventual ee_A and dr of the total reaction. The observed values for r_α across multiple reactions were calculated in the range of 40 to 55%, an observation that suggests an unanticipated amount of cyclohexanone product **295** is produced during the final alkylation of enolate **292**. Notably, this low selectivity and undesired accumulation of diallyl product **295** has no impact upon ee_A, which remains large for all reactions examined. However, because this second alkylation occurs with lower efficiency than desired, the formation of cyclohexanone **295** at the expense of desired product **294** leads to a reduction in dr. Interestingly, these findings suggest the disappointing diastereomeric ratios observed for some of our double alkylation reactions are partly due to ineffective catalyst control at the second stage of bond formation, a conclusion that contradicts our earlier experiments employing enantioenriched β-ketoester substrates.

An additional experiment to further investigate the impact of the primary and secondary alkylation selectivities in these reactions would help resolve this observed contradiction. In particular, performing an alkylation from an enol carbonate substrate in the presence of a racemic β-ketoester stereocenter would provide an excellent system to probe the selectivity of the primary alkylation process. Starting from known β-ketoester **298**, hydrogenation of the allyl group, followed by methylation of the α-position, will afford cyclohexanone **299**. After installation of an appropriate enol carbonate moiety to achieve carbonate-ester substrate **300**, this material will be subjected to the conditions of

the stereoselective catalytic alkylation to ultimately generate β-ketoester **301**. By measuring the resulting dr of propyl ester **301**, data complementary to that observed in the alkylation of β-ketoester **287** (Scheme 3.21) will be attained, thus providing access to a more complete set of data for the process of double stereoselective alkylation. If a dr near 1 : 1 is observed for this proposed reaction, the evidence would suggest that the primary alkylation proceeds with very high catalyst control. If the value of dr is observed to deviate significantly from a 1 : 1 ratio, this result would imply considerable substrate interference with catalyst activity and consequent low selectivity for the primary alkylation.

Scheme 3.25 Experiment proposed for further investigation of double asymmetric alkylation

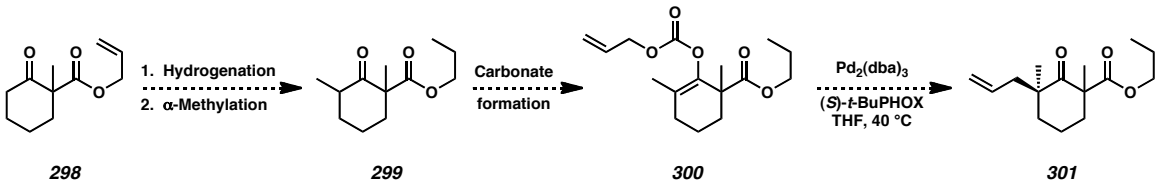

It should be noted that the studies conducted above exclusively focused on the 2,6-substituted substrates that react to form diallyl cyclohexanone **224**. Many of the conclusions concerning these experiments may be specific to double alkylation reactions of compounds with similar substitution patterns.

3.4 CONCLUSION

Multiple asymmetric transformations are powerful techniques that rapidly build molecular complexity via the concurrent installation of two or more stereocenters under

catalyst or reagent control. By leveraging these versatile reactions, not only is it possible to efficiently construct structurally difficult compounds, but it is also possible to garner an impressive boost in the *ee* of the desired product via statistical amplification. Indeed, multiple asymmetric reactions are able to produce very high levels of enantioenrichment in the major diastereomer of reaction. This is largely because the minor diastereomer produced in the course of such a transformation serves as a "buffer" against accumulation of the opposite enantiomer of the major diastereomer. Thus, high values attained for *ee* in these reactions are always accompanied by lower than anticipated diastereomeric ratios.

While multiple asymmetric transformations are powerful tools with which to approach a variety of synthetic challenges, their optimization is often made cumbersome due to the difficulty of analyzing multiple, convoluted reaction pathways. However, depending on the degree to which substrate interference impacts catalyst control, a wide variety of simplified mathematical representations are available for the extraction of crucial selectivity data from the values of ee_A, ee_B, and dr. By appealing to expressions most suitable for the situations in question, our group has been able to deconstruct the various stages of a double asymmetric alkylation. In so doing, we found that the secondary alkylation process is prone to experience deleterious catalyst-substrate interactions. This valuable data has provided valuable insight into the behavior of the reaction, and further refinement of our technology based on these findings is currently underway.

3.5 EXPERIMENTAL SECTION

3.5.1 MATERIALS AND METHODS

All reactions were performed at ambient temperature (22 °C) unless otherwise noted. Reactions requiring external heat were modulated to the specified temperatures indicated by using an IKAmag temperature controller. All reactions were performed in glassware flame dried under vacuum and allowed to cool under nitrogen or argon. Solvents were dried by passage over a column of activated alumina with an overpressure of argon gas. Tetrahydrofuran was distilled directly over benzophenone and sodium, or else was dried by passage over a column of activated alumina with an overpressure of argon gas. (*S*)-*t*-BuPHOX (**193**) was prepared according to known methods.[33,34] All other chemicals and reagents were used as received. Compounds purified by flash chromatography utilized ICN silica gel (particle size 0.032-0.063 mm) or SiliCycle® Silia*Flash*® P60 Academic Silica Gel (particle size 40-63 μm; pore diameter 60 Å). Thin-layer chromatography (TLC) was performed using E. Merck silica gel 60 F254 pre-coated plates (0.25 mm) and visualized by UV, *p*-anisaldehyde, or alkaline permanganate staining. NMR spectra were recorded on a Varian Mercury 300 (at 300 MHz for ^{1}H NMR and 75 MHz for ^{13}C), Varian Inova 500 (at 500 MHz for ^{1}H NMR and 125 for ^{13}C), or Varian Inova 600 (at 600 MHz for 1H NMR only) instrument, and are reported relative to residual $CHCl_3$ (δ 7.26 for ^{1}H NMR, δ 77.16 for ^{13}C) or C_6H_6 (δ 7.16 for ^{1}H NMR, δ 128.06 for ^{13}C). The following format is used for the reporting of ^{1}H NMR data: chemical shift (δ ppm), multiplicity, coupling constant (Hz), and integration. Data for ^{13}C NMR spectra are reported in terms of chemical shift. IR spectra were recorded on a Perkin Elmer

Spectrum Paragon 1000 spectrometer, and data are reported in frequency of absorption (cm^{-1}). High-resolution mass spectra were obtained from the Caltech Mass Spectral Facility, or else were acquired using an Agilent 6200 Series TOF mass spectrometer with an Agilent G1978A Multimode source in ESI, APCI, or MM (ESI/APCI) ionization mode. Analytical chiral gas chromatography was performed with an Agilent 6850 GC using a G-TA (30 m x 0.25 mm) column (1.0 mL/min carrier gas flow). Analytical achiral gas chromatography was performed with an Agilent 6850 GC using a DB-WAX (30 x 0.25 mm) column (1.0 mL/min carrier gas flow). Analytical chiral super critical fluid chromatography was performed with a Mettler supercritical CO_2 analytical chromatography system equipped with a CTC analytics HTC PAL autosampler, utilizing a Chiracel OD/OD-H column with a flow rate of 2.5 mL/min. Analytical chiral super critical fluid chromatography runs were visualized with a UV-visible detector operating at 210 nm. Automated experiments were performed with a Symex Core Module while inside a nitrogen-filled glovebox. Optical rotations were measured with a Jasco P-1010 polarimeter at 589 nm using a 100 mm path-length cell.

3.5.2 PREPARATIVE PROCEDURES

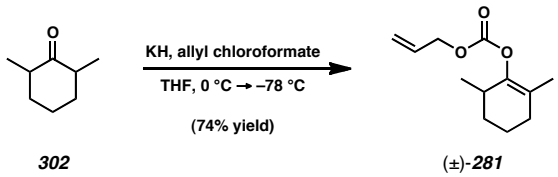

302 (±)-***281***

Enol Carbonate (281). To a flame dried flask under argon was added KH (30% in mineral oil, 0.552 g, 4.13 mmol, 1.04 equiv). The KH was suspended in dry hexanes (ca. 6.5 mL), stirred briefly, and then the hexanes were removed via syringe without disturbing the KH sediment. This process was repeated two additional times, and the residual solid was then dried under high vacuum for 10 min. The washed KH powder was then suspended in THF (12.5 mL) and cooled to 0 °C. Once cooled, 2,6-dimethylcyclohexanone (**302**, 0.500 mL, 3.96 mmol, 1.00 equiv) was added dropwise via syringe. The reaction was allowed to slowly reach room temperature, and then was allowed to deprotonate over 10 h. After this time had elapsed, the reaction was cooled to –78 °C, and a single portion of allyl chloroformate (0.430 mL, 4.05 mmol, 1.02 equiv) was added dropwise. After a further 15 min of reaction at –78 °C, the flask was allowed to reach room temperature. The reaction was quenched via the addition of saturated $NH_4Cl_{(aq)}$ (10 mL), and the phases were thereafter separated. The aqueous phase was extracted with Et_2O (4 x 20 mL). The combined organic layers were washed with brine (20 mL), dried over $MgSO_4$, filtered, and then concentrated in vacuo. The resulting material was thereafter purified over silica gel using 2% ethyl acetate in hexanes as eluent. This afforded (±)-**281** as a clear, colorless oil (0.619 g, 74% yield): ^{1}H NMR (500 MHz, $CDCl_3$) δ 5.96 (app ddt, J = 17.2, 10.5, 5.7 Hz, 1H), 5.38 (app dq, J = 17.2, 1.5 Hz, 1H), 5.28 (app dq, J = 10.5, 1.2 Hz, 1H), 4.66 (ddd, J = 5.7, 2.6, 1.2 Hz, 2H),

2.52–2.42 (m, 1H), 2.07–2.01 (m, 2H), 1.86 (dddd, J = 12.8, 8.8, 8.5, 3.1 Hz, 1H), 1.66 (app dddt, J = 17.7, 9.0, 6.0, 3.1 Hz, 1H), 1.61–1.52 (m, 1H), 1.56–1.55 (m, 3H), 1.45–1.37 (m, 1H), 1.02 (d, J = 7.0 Hz, 3H); ^{13}C NMR (125 MHz, $CDCl_3$) δ 153.3, 146.1, 131.7, 121.3, 118.9, 68.7, 31.9, 31.4, 30.8, 20.1, 18.3, 16.2; IR (Neat film, NaCl) 2934, 2875, 1756, 1701, 1650, 1455, 1366, 1292, 1248, 1156, 1132, 1035, 994, 981, 940 cm^{-1}; HRMS (EI) *m/z* calc'd for $C_{12}H_{18}O_3$ $[M]^+$: 210.1256, found 210.1259.

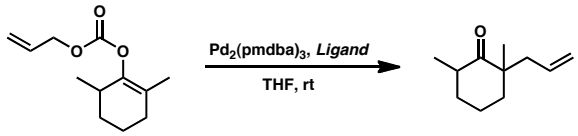

(±)-***281*** ***282***

Cyclohexanone (282). A representative procedure for the synthesis of cyclohexanone **282** is as follows: To a flame dried flask under argon was added 0.004 g $Pd_2(pmdba)_3$ (0.004 g, 0.004 mmol, 0.025 equiv) and a corresponding amount (0.009 mmol, 0.06 equiv) of a given PHOX ligand derivative. These solids were briefly vacuum purged in the flask, before being backfilled with argon. To these solids was added a single portion of THF (4.3 mL), and the reaction was allowed to pre-complex over 30 min. After this time had elapsed, the reaction was treated with neat enol carbonate (±)-**281** (0.030g, 0.143 mmol, 1.00 equiv). The reaction was allowed to proceed for 3 h. The solvent was then removed in vacuo, and the resulting crude material was purified directly over silica using 1% Et_2O in pentane as eluent. Cyclohexanone **282** was isolated as a clear oil (inseparable mixture of diastereomers): Chiral GC assay (GTA column): 90 °C isothermal method over 40 min, t_r (Enantiomer A, diastereomer A) = 25.3 min; t_r (Enantiomer B, diastereomer A) = 26.7 min; t_r (Enantiomer A, diastereomer B) = 27.5

min; t_r (Enantiomer B, diastereomer B) 32.0 min. ^{1}H NMR (500 MHz, $CDCl_3$) δ 5.60 (dddd, *J* = 14.7, 13.7, 9.5, 7.4 Hz, 1H), 5.07–4.98 (comp. m, 2H), 2.65–2.56 (m, 1H), 2.53 (dd, *J* = 13.9, 7.4 Hz, 1H), 2.52–2.21 (m, 1H), 2.17 (dd, *J* = 13.9, 7.4 Hz, 1H), 2.09–2.00 (m, 1H), 1.97–1.82 (m, 1H), 1.74–1.56 (m, 1H), 1.53–1.45 (m, 1H), 1.38–1.28 (m, 1H), 1.01 (s, 3H), 0.99 (d, *J* = 6.5 Hz, 3H); ^{13}C NMR (125 MHz, $CDCl_3$) δ 216.5, 133.3, 118.1, 48.9, 41.9, 41.5, 40.0, 36.8, 22.7, 21.2, 15.1; IR (Neat film, NaCl) 3077, 2969, 2931, 2870, 2854, 1706, 1640, 1456, 1377, 1316, 1126, 999, 958, 914, 856 cm^{-1}; HRMS (EI) *m/z* calc'd for $C_{11}H_{18}O$ $[M]^+$: 166.1358, found 116.1357; $[\alpha]^{25}_D$ –21.2 (*c* 1.14, CH_2Cl_2).

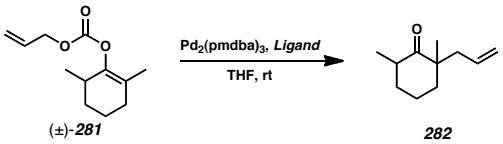

Ligand	ee_A (%)	ee_B (%)	*de* (%)	dr (X : 1)	r_α (%)	r_β (%)
PPh_3	-	-	63.6	4.5	63.6	–63.6
dppp	-	-	42.4	2.5	42.6	–42.6
284	-	-	92.1	24	92.1	–92.1
193	40.2	98.9	46.2	2.7	99.4	10.0
303	–39.5	–98.9	50.1	3.0	–4.4	–99.5
304	22.2	96.3	66.5	5.0	98.8	–32.6
305	38.6	97.1	46.1	2.7	98.5	8.5
286	5.9	78.0	87.8	15	97.3	–78.1
306	–13.0	–88.5	85.7	13	71.5	–98.5
285	35.9	78.8	37.6	2.2	86.8	11.7
307	45.8	87.1	56.2	3.6	95.1	–1.6
308	–35.3	–81.8	57.1	3.7	13.2	–92.9
309	17.4	90.7	73.3	6.5	97.6	–46.5
310	–15.6	–76.1	71.5	6.0	48.5	–93.3

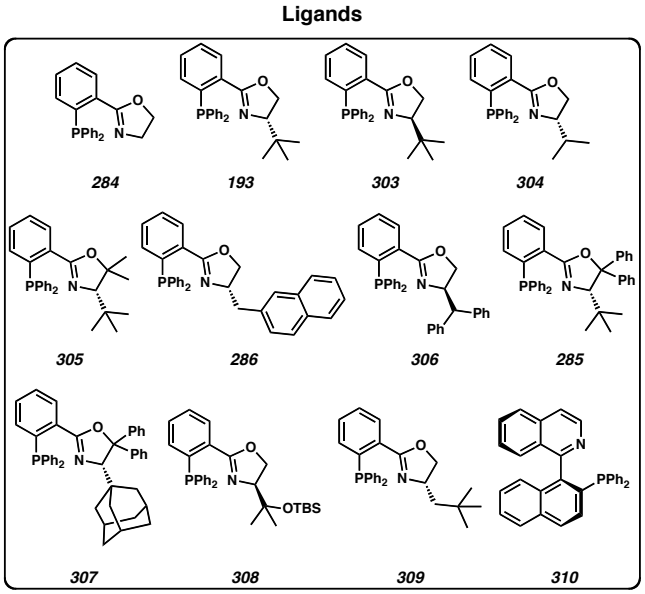

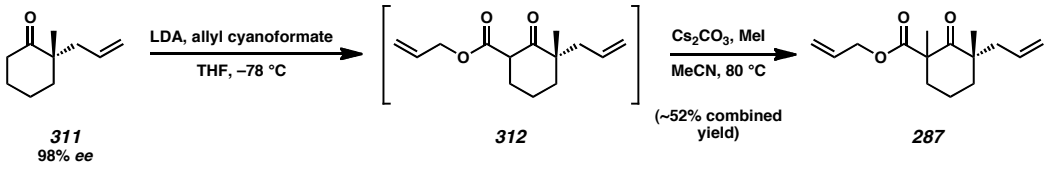

β-ketoester (287). To a flame dried flask was added THF (50 mL) and diisopropyl amine (1.76 mL, 12.3 mmol, 1.25 equiv). This solution was cooled to 0 °C, before being treated with *n*-BuLi (5.14 mL, 2.3 M in hexanes, 11.8 mmol, 1.20 equiv). The solution was allowed to stir for 30 min at this temperature, before being cooled to –78 °C. After this temperature was reached, neat cyclohexanone **311** (1.50 g, 9.85 mmol, 1.00 equiv) was added dropwise. Deprotonation was allowed at –78 °C over 30 min, after which time the reaction was treated with a single portion of neat allyl cyanoformate (1.42 mL, 12.8 mmol, 1.30 equiv). The reaction was allowed to slowly reach room temperature by warming in the bath over 6 h. After the reaction had reached room temperature it was quenched via the addition of saturated $NH_4Cl_{(aq)}$ (30 mL). The phases were separated, and the aqueous layer was extracted with ethyl acetate (3 x 40 mL). Combined organics were washed with brine (40 mL), dried over $MgSO_4$, and filtered. The material resultant from this process was passed over a plug of silica using 20% ethyl acetate in hexanes as eluent, and then was used directly in the next reaction.

To a flame dried Schlenk flask was added Cs_2CO_3 (3.89 g, 11.8 mmol, 1.20 equiv). This material was vacuum purged briefly, before being backfilled with nitrogen. To this flask was added 50 mL of MeCN containing the crude product of the previous sequence (ca. 2.33g, 9.85 mmol, 1.00 equiv). The reaction was treated with MeI (1.90 mL, 30.5 mmol, 3.10 equiv) and the reaction vessel was sealed. The reaction was then heated to 80 °C for 12 h. After this time had elapsed, the reaction was cooled to room temperature and filtered to remove excess solid Cs_2CO_3. The filtrate was diluted with saturated

$NH_4Cl_{(aq)}$ (40 mL) and the two phases were then separated. The aqueous phase was extracted with ethyl acetate (4 x 20 mL), and the combined organic phases were washed with brine (40 mL). The organic layers were dried over $MgSO_4$, filtered, and concentrated in vacuo. The resulting material was purified twice over silica using a gradient of 0 → 5% Et_2O in pentane as eluent. This afforded β-ketoester **287** as a mixture of diasteromers, isolated as a clear, colorless oil (1.28 g, 52% combined yield). Analytically pure samples of each diastereomer were obtained via preparatory HPLC separation, using 0 → 3.5% *tert*-butyl methyl ether.

Diastereomer A: ^{1}H NMR (500 MHz, $CDCl_3$) δ 5.87 (app ddt, *J* = 17.2, 10.4, 5.8 Hz, 1H), 5.75 (dddd, *J* = 17.2, 10.2, 7.6, 7.1 Hz, 1H), 5.30 (app dq, *J* = 17.2, 1.5 Hz, 1H), 5.22 (app dq, *J* = 10.4, 1.2 Hz, 1H), 5.03 (app dddt, *J* = 18.4, 17.0, 2.5, 1.1 Hz, 2H), 4.61 (app ddt, *J* = 13.2, 5.8, 1.4 Hz, 1H), 4.52 (app ddt, *J* = 13.2, 5.8, 1.4 Hz, 1H), 2.55–2.50 (m, 1H), 2.29 (app ddt, *J* = 13.8, 7.0, 1.1 Hz, 1H), 2.25–2.19 (m, 1H), 2.01–1.90 (m, 1H), 1.68–1.60 (comp. m, 3H), 1.45–1.38 (m, 1H), 1.32 (s, 3H), 1.04 (s, 3H); ^{13}C NMR (125 MHz, $CDCl_3$) δ 210.9, 172.6, 134.7, 131.6, 118.9, 118.1, 65.9, 55.5, 49.0, 43.7, 37.4, 36.7, 23.7, 23.6, 18.4; IR (Neat film, NaCl) 3076, 2978, 2937, 1738, 1706, 1639, 1459, 1377, 1237, 1204, 1175, 1141, 1062, 994, 917 cm^{-1}; HRMS (EI) *m/z* calc'd for $C_{15}H_{22}O_3$ $[M+H]^+$: 251.1642, found 251.1642; $[\alpha]^{25}_D$ –97.6 (*c* 0.61, CH_2Cl_2). **Diastereomer B**: ^{1}H NMR (500 MHz, $CDCl_3$) δ 5.87 (app ddt, *J* = 17.2, 10.4, 5.8 Hz, 1H), 5.61 (dddd, *J* = 16.8, 10.2, 7.9, 6.5 Hz, 1H), 5.31 (app dq, *J* = 17.2, 1.5 Hz, 1H), 5.23 (ddd, *J* = 10.4, 2.5, 1.2 Hz, 1H), 5.07–4.98 (m, 2H), 4.64 (app ddt, *J* = 13.1, 5.8, 1.4 Hz, 1H), 4.48 (app ddt, *J* = 13.1, 5.8, 1.4 Hz, 1H), 2.52 (app dtd, *J* = 13.8, 4.5, 2.1 Hz, 1H), 2.24–2.15 (m, 2H), 2.00–1.90 (m, 1H), 1.85 (dddd, *J* = 13.9, 6.0, 4.1, 2.1 Hz, 1H), 1.66–1.59 (m, 1H), 1.51

(dddd, J = 13.8, 11.1, 6.3, 4.5 Hz, 2H), 1.35 (s, 3H), 1.04 (s, 3H); ^{13}C NMR (125 MHz, $CDCl_3$) δ 211.3, 172.5, 133.8, 131.6, 119.1, 118.4, 66.0, 55.6, 48.9, 41.9, 37.4, 36.4, 24.1, 23.9, 18.0; IR (Neat film, NaCl) 2935, 2874, 1734, 1705, 1456, 1377, 1241, 1169, 1145, 1118, 1080, 994, 974, 918, 868 cm^{-1}; HRMS (EI) *m/z* calc'd for $C_{15}H_{22}O_3$ $[M+H]^+$: 251.1642, found 251.1643; $[\alpha]^{25}_D$ +51.7 (*c* 0.80, CH_2Cl_2).

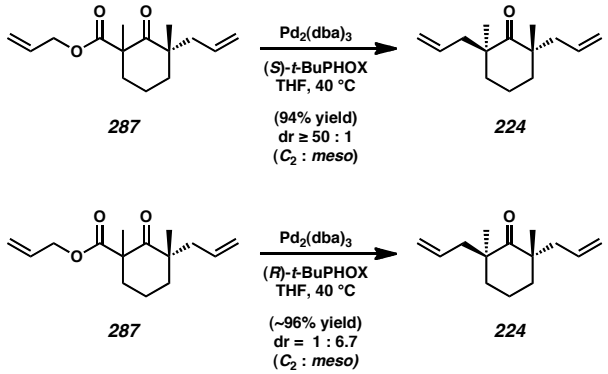

Diallyl cyclohexanone (224). To a flame dried flask under argon was added $Pd_2(dba)_3$ (0.003 g, 0.004 mmol, 0.04 equiv) and of either (*R*) or (*S*)-*t*-BuPHOX (0.003 g, 0.008 mmol, 0.08 equiv). These solids were briefly vacuum purged in the flask before being backfilled with argon. To these solids were added 3 mL of THF, and the reaction was allowed to precomplex at 40 °C over 30 min. After this time had elapsed, the reaction was treated with a single portion of neat β-ketoester **287** (0.025 g, 0.100 mmol, 1.00 equiv). The reaction was allowed to proceed for 3 h. The solvent was then removed in vacuo, and the resulting crude material was purified directly over silica using 2% Et_2O in pentane as eluent. This afforded cyclohexanone **224** as a clear, colorless oil (19.3 mg, 94% yield). Characterization data was identical to that reported in reference 3: ^{1}H NMR (300 MHz, $CDCl_3$) δ 5.65 (m, 2H), 5.10–4.95 (m, 4H), 2.33 (dd, J = 13.8, 6.9 Hz, 2H), 2.18 (dd, J = 13.8, 7.8 Hz, 2H), 1.87–1.68 (m, 4H), 1.59–1.48 (m, 2H), 1.06 (s, 6H); ^{13}C

NMR (75 MHz, $CDCl_3$) δ 218.6, 134.4, 118.0, 47.6, 43.9, 36.4, 25.0, 17.3; IR (Neat film, NaCl) 3076, 2930, 1694, 1639, 1461, 1374, 992, 914 cm^{-1}; HRMS (EI) *m/z* calc'd for $C_{14}H_{22}O$ $[M]^+$: 206.1671, found 206.1675; $[\alpha]^{25}_D$ –54.0 (*c* 0.95, hexane).

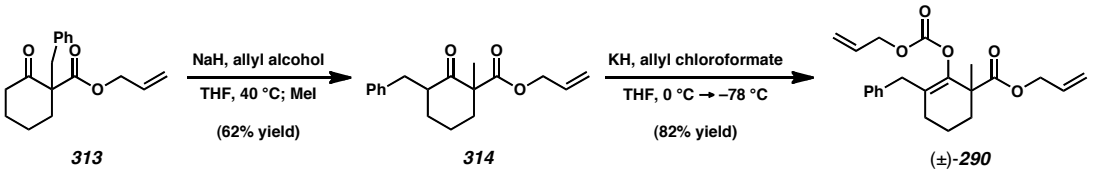

313 ***314*** (±)-***290***

Enol carbonate (290). To a flame dried vial under argon was added NaH (60% in mineral oil, 0.299 g, 7.48 mmol, 2.04 equiv) and THF (20 mL). This suspension was cooled to 0 °C, and then was treated with allyl alcohol (0.550 mL, 8.09 mmol, 2.20 equiv). After gas evolution had halted the reaction was treated with neat cyclohexanone **313** (1.00 g, 3.67 mmol, 1.0 equiv) and was heated to 40 °C. After stirring for 3 h at 40 °C, the reaction was cooled to room temperature and treated with a single portion of MeI (0.510 mL, 8.19 mmol, 2.23 equiv). The reaction was thereafter heated to 40 °C for an additional 12 h. After this time had elapsed, the reaction was cooled to room temperature and quenched with saturated $NH_4Cl_{(aq)}$ (40 mL). The phases were separated, and the aqueous layer was extracted with Et_2O (3 x 20 mL). The combined organic layers were washed with brine (40 mL), dried over $MgSO_4$ and filtered. After removal of the solvent in vacuo, the crude material obtained was purified over silica gel using 3% ethyl acetate in hexanes. Because the resulting material isolated was not of sufficient purity for characterization, this mixture of diasteromeric β-ketoesters was carried into the next transformation directly.

To a flame dried flask under argon was added KH (30% in mineral oil, 0.280 g, 2.09 mmol, 1.20 equiv). The KH was suspended in dry hexanes (ca. 4.0 mL), stirred briefly, and then was allowed to settle. The hexanes layer was carefully removed via syringe while taking precautions not to disturb the KH sediment. This process was repeated two additional times, and the residual solid was then dried under high vacuum for 10 min. The washed KH powder was then suspended in THF (5.8 mL). To this was added, dropwise via syringe, the material obtained from the preceding step (ca. 0.500 g, 1.75 mmol, 1.0 equiv). The reaction was allowed to deprotonate at room temperature over 1 h. After this time had elapsed, the reaction was cooled to –78 °C, and a single portion of allyl chloroformate (0.222 mL, 2.10 mmol, 1.20 equiv) was added dropwise. After a further 1.5 h of reaction at –78 °C, the flask was allowed to reach room temperature. The reaction was quenched via the addition of saturated $NH_4Cl_{(aq)}$ (10 mL), and the phases were separated. The aqueous phase was extracted with Et_2O (4 x 20 mL). The combined organic layers were washed with brine (20 mL), dried over $MgSO_4$, filtered, and then concentrated in vacuo. The resulting material was thereafter purified over silica gel using 5% ethyl acetate in hexanes as eluent. This afforded **290** as a clear, colorless oil (0.530 g, 51% yield from **313**). ^{1}H NMR (500 MHz, $CDCl_3$) δ 7.28–7.24 (comp. m, 2H), 7.22–7.17 (comp. m, 3H), 5.93 (app dddt, *J* = 17.2, 10.4, 5.7, 2.8 Hz, 2H), 5.35 (app ddq, *J* = 17.2, 12.2, 1.5 Hz, 2H), 5.25 (app ddq, *J* = 14.3, 10.5, 1.3 Hz, 2H), 4.65–4.60 (m, 4H), 3.41 (d, *J* = 14.9 Hz, 1H), 3.19 (d, *J* = 14.9 Hz, 1H), 2.20–2.14 (m, 1H), 2.01–1.98 (m, 2H), 1.67–1.59 (comp. m, 3H), 1.40 (s, 3H); ^{13}C NMR (125 MHz, $CDCl_3$) δ 174.8, 153.6, 143.1, 138.9, 132.3, 131.5, 129.1, 128.5, 127.7, 126.3, 119.3, 118.1, 69.0, 65.8, 47.2, 36.8, 36.1, 28.2, 22.5, 19.3; IR (Neat film, NaCl) 3026, 2942, 1759, 1733, 1649,

1602, 1496, 1434, 1365, 1238, 1166, 1108, 1024, 994, 940 cm^{-1}; HRMS (EI) *m/z* calc'd for $C_{22}H_{26}O_5$ $[M]^+$: 370.1780, found 370.1788.

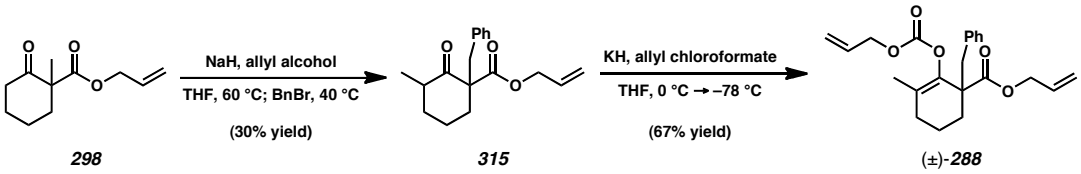

298 ***315*** (±)-***288***

Enol carbonate (288). To a flame dried vial under argon was added NaH (60% in mineral oil, 1.05 g, 26.3 mmol, 2.07 equiv) and THF (64 mL). This suspension was cooled to 0 °C, and then was treated with allyl alcohol (3.12 mL, 46.2 mmol, 3.64 equiv). After gas evolution had halted, the reaction was treated with neat cyclohexanone **298** (2.50 g, 12.7 mmol, 1.0 equiv) and was heated to 60 °C. After stirring for 12 h at 60 °C, the reaction was cooled to 40 °C and treated with neat BnBr (3.20 mL, 26.9 mmol, 2.12 equiv). The reaction was stirred at 40 °C for three additional hours, but complete conversion was not observed. An additional portion of BnBr (2.0 mL, 16.8 mmol, 1.33 equiv) was introduced to the flask, and the reaction was allowed to continue for 12 h more. After this time had elapsed, the reaction was cooled to room temperature and quenched with saturated $NH_4Cl_{(aq)}$ (40 mL). The phases were separated, and the aqueous layer was extracted with Et_2O (3 x 40 mL). The combined organic layers were washed with brine (40 mL), dried over $MgSO_4$, and were filtered. After removal of the solvent in vacuo, the crude material obtained was purified over silica gel using 3% ethyl acetate in hexanes. Because the resulting material isolated was not of sufficient purity for characterization, this mixture of diasteromeric β-ketoesters was carried into the next transformation directly.

To a flame dried flask under argon was added KH (30% in mineral oil, 0.291 g, 2.18 mmol, 1.24 equiv). The KH was suspended dry hexanes (ca. 4.0 mL), stirred briefly, and then was allowed to settle. The hexanes layer was carefully removed via syringe while taking precautions not to disturb the KH sediment. This process was repeated two additional times, and the residual solid was then dried under high vacuum for 10 min. The washed KH powder was then suspended in THF (6.0 mL). To this suspension was added, dropwise via syringe, the material obtained from the preceding step (ca. 0.500 g, 1.75 mmol, 1.0 equiv). The reaction was allowed to deprotonate at room temperature over 5 h. After this time had elapsed, the reaction was cooled to –78 °C, and a single portion of allyl chloroformate (0.225 mL, 2.10 mmol, 1.20 equiv) was added dropwise. After a further 4 h of reaction at –78 °C, the flask was allowed to reach room temperature. The reaction was quenched via the addition of saturated $NH_4Cl_{(aq)}$ (10 mL), and the phases were separated. The aqueous phase was extracted with Et_2O (4 x 25 mL). The combined organic layers were washed with brine (20 mL), dried over $MgSO_4$, filtered, and concentrated in vacuo. The resulting material was purified over silica gel using 5% ethyl acetate in hexanes as eluent. This afforded **288** as a clear, colorless oil (0.493 g, 20% yield from **298**). ^{1}H NMR (500 MHz, $CDCl_3$) δ 7.25–7.18 (comp. m, 3H), 7.16–7.13 (comp. m, 2H), 5.95 (app dddt, *J* = 34.7, 17.2, 10.5, 5.7 Hz, 2H), 5.42 (app dq, *J* = 17.2, 1.5 Hz, 1H), 5.34 (app dq, *J* = 17.2, 1.5 Hz, 1H), 5.30 (app dq, *J* = 10.5, 1.3 Hz, 1H), 5.23 (app dq, 10.5, 1.3 Hz, 1H), 4.67 (app ddt, *J* = 12.2, 5.8, 1.4 Hz, 1H), 4.64–4.60 (comp. m, 2H), 4.49 (app ddt, *J* = 13.4, 5.8, 1.4 Hz, 1H), 3.30 (d, *J* = 13.5 Hz, 1H), 3.02 (d, *J* = 13.5 Hz, 1H), 2.13–1.92 (comp. m, 3H), 1.78–1.68 (m, 1H), 1.58 (s, 3H), 1.58–1.54 (m, 1H), 1.49–1.41 (m, 1H); ^{13}C NMR (125 MHz, $CDCl_3$) δ 172.9, 152.7, 140.3,

137.0, 132.3, 131.8, 130.6, 128.1, 127.7, 126.7, 119.1, 118.2, 68.9, 65.9, 50.9, 41.9, 31.3, 30.9, 19.4, 17.4; IR (Neat film, NaCl) 3029, 2942, 1761, 1732, 1649, 1604, 1496, 1454, 1365, 1230, 1176, 1155, 1094, 1032, 993, 937 cm^{-1}; HRMS (EI) *m/z* calc'd for $C_{22}H_{26}O_5$ $[M]^+$: 370.1780, found 370.1770.

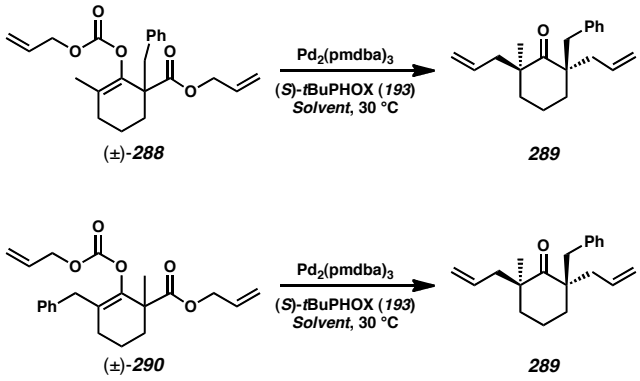

Diallyl cyclohexanone (289). The following series of experiments were run simultaneously inside of a glovebox under a nitrogen atmosphere. To each of 48 vials in two 24-well plates was added solution of $Pd_2(pmdba)_3$ (62.5 μL, 3.60 mM in THF, 0.225 μmol, 0.025 equiv). The solvent was removed from the vials in vacuo, and to each vial was added of (*S*)-*t*-BuPHOX in a (20 μL, 27.9 mM solution of a 1 : 1 mixture of PhMe : Hex, 0.559 μmol, 0.062 equiv). To each vial was then added a portion of the appropriate solvent (160 μL) to be used in the solvent screen. Each vial was then allowed to stir for 40 min at 30 °C in order to allow the palladium and ligand to precomplex. After this time had elapsed, either **289** or **290** (20 μL, 0.450 M solution of a 1 : 1 mixture of PhMe : Hex, 8.99 μmol) were added to each vial. Each of the 24 vials of the first plate (Plate A) were charged with **288**. Each of the 24 vials of the second plate (Plate B) were charged with **290**. The vials were then treated with an additional volume of solvent such that the

first 12 vials of each plate achieved a final concentration of 0.03 M, while the last twelve vials of each plate achieved a final concentration of 0.01 M. All reactions were tightly capped, and then run for 70 h at 30 °C inside the glovebox. After this time had elapsed, each reaction was passed over a small plug of silica using Et_2O as eluent. Afterward all solvents were removed in vacuo, and each reaction was assayed by ^1H NMR and analytical SFC. Values for *ee* and dr were collected via analytical supercritical fluid chromatography over a Chiralcel OD/OD-H column at a flow rate of 2.5 mL/min using an isocratic elution of 3% *i*-PrOH in CO_2: t_r (major diastereomer, major enantiomer) = 7.8 min; t_r (minor diastereomer, minor enantiomer) = 8.5 min; t_r (major diastereomer, minor enantiomer) = 9.2 min; t_r (minor diastereomer, major enantiomer) = 9.8 min. ^1H NMR (500 MHz, $CDCl_3$) δ 7.27–7.17 (comp. m, 3H), 7.12–7.09 (m, 2H), 5.76–5.62 (m, 1H), 5.58–5.49 (m, 1H), 5.12–5.08 (m, 1H), 5.08–5.01 (m, 1H), 4.99–4.93 (m, 2H), 3.15 (d, *J* = 13.3 Hz, 1H), 2.52 (d, *J* = 13.3 Hz, 1H), 2.39 (dd, *J* = 14.1, 7.0, 1H), 2.29 (dd, *J* = 13.7, 6.7 Hz, 1H), 2.20 (dd, *J* = 14.0, 7.5 Hz, 1H), 2.07 (dd, *J* = 13.7, 8.0, 1H), 1.80–1.59 (comp. m, 4H), 1.55–1.39 (comp. m, 2H), 1.09 (s, 3H); ^{13}C NMR (125 MHz, $CDCl_3$) δ 217.9, 138.0, 134.6, 134.3, 131.4, 128.0, 126.4, 118.5, 118.1, 52.6, 47.5, 44.2, 42.8, 42.6, 35.5, 32.1, 25.6, 17.3; IR (Neat film, NaCl) 3075, 2933, 2869, 1692, 1638, 1496, 1454, 1373, 1072, 994, 916, 743 cm^{-1}; HRMS (EI) *m/z* calc'd for $C_{20}H_{26}O$ $[M]^+$: 282.1984, found 282.1972; $[\alpha]^{25}_D$ –8.6 (*c* 1.05, CH_2Cl_2).

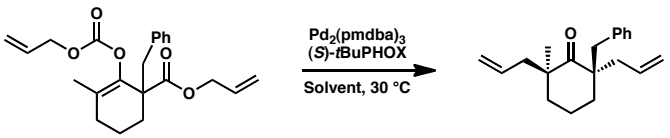

(±)-***288*** ***289***

0.03 M Concentration

Solvent	ee_A (%)	ee_B (%)	*de* (%)	dr (X : 1)	yield lost (%)	r (%)	r_α (%)	r_β (%)
Dioxane	50.2	62.3	47.4	2.8	26.3	53.4	44.3	–57.4
DME	83.3	88.3	44.4	2.6	27.8	84.7	43.4	–57.5
Et_2O	92.7	83.9	66.1	4.9	16.9	91.2	67.4	–37.9
Et_2O / Hex	93.4	79.4	69.7	5.6	15.2	91.3	71.6	–28.4
PhH	87.4	82.5	59.2	3.9	20.4	86.4	60.0	–47.5
PhF	76.2	88.1	35.5	2.1	32.3	80.0	32.6	–61.5
PhMe	91.4	81.1	63.6	4.5	18.2	92.6	65.3	–34.4
PhMe / Hex	91.2	79.3	68.7	5.4	15.6	89.3	70.4	–39.3
t-BuOMe	90.8	82.8	61.5	4.2	19.2	89.3	62.9	–38.4
THF[a]	86.6	85.6	44.4	2.6	27.8	86.3	44.7	–41.5
THF[b]	84.7	83.6	42.9	2.5	28.6	84.4	43.1	–40.0
THF / Hex[a]	68.0	48.9	70.1	5.7	14.9	65.1	73.1	–56.2

0.01 M Concentration

Solvent	ee_A (%)	ee_B (%)	*de* (%)	dr (X : 1)	yield lost (%)	r (%)	r_α (%)	r_β (%)
Dioxane	57.4	62.3	45.9	2.7	27.0	58.7	44.7	–57.4
DME	82.9	84.4	41.2	2.4	29.4	83.3	40.8	–44.9
Et_2O	95.6	71.6	65.5	4.8	17.2	91.5	69.1	14.7
Et_2O / Hex	89.6	93.2	72.2	6.2	13.9	90.1	71.8	–80.9
PhH	91.9	80.1	54.5	3.4	22.7	89.2	56.7	–16.1
PhF	71.6	83.2	41.1	2.4	29.4	75.0	38.4	–60.5
PhMe	90.4	71.7	62.2	4.3	18.9	86.9	65.3	–18.7
PhMe / Hex	92.5	76.5	70.1	5.7	14.9	90.1	72.3	–29.1
t-BuOMe	91.1	85.3	59.2	3.9	20.4	89.9	60.2	–40.5
THF[a]	80.9	89.3	44.4	2.6	27.8	83.2	42.3	–64.5
THF[b]	86.8	84.2	47.4	2.8	26.3	86.1	47.9	–40.1
THF / Hex[a]	91.0	85.2	61.5	4.2	19.2	89.9	62.5	–43.7

[a] The THF employed in these reactions was dried by passing the solvent over a column of activated alumina with an argon overpressure. [b] The THF employed in these reactions was dried via distillation over benzophenone and sodium metal.

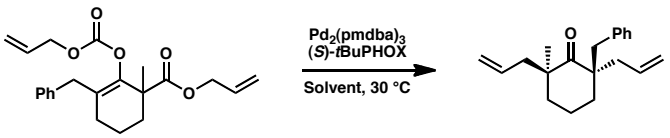

(±)-***290*** ***289***

0.03 M Concentration

Solvent	ee_A (%)	ee_B (%)	*de* (%)	dr (X : 1)	yield lost (%)	r (%)	r_α (%)	r_β (%)
Dioxane	66.2	76.1	23.1	1.6	38.5	67.5	19.1	–43.4
DME	93.4	86.1	31.0	1.9	34.5	90.9	32.8	5.1
Et_2O	89.5	63.7	45.9	2.7	27.0	82.5	51.5	12.3
Et_2O / Hex	92.4	58.9	50.0	3.0	25.0	84.0	56.8	28.6
PhH	92.5	81.7	48.7	2.9	25.6	89.7	50.9	–7.8
PhF	87.9	86.2	20.0	1.5	40.0	87.2	20.4	–13.6
PhMe	94.3	87.0	52.4	3.2	23.8	92.6	53.8	–16.8
PhMe / Hex	92.1	90.4	54.5	3.4	22.7	91.7	54.9	–47.3
t-BuOMe	91.6	79.9	44.4	2.6	27.8	88.4	46.9	–4.1
THF[a]	90.6	93.2	37.5	2.2	31.3	91.4	36.9	–50.5
THF[b]	88.8	88.4	37.5	2.2	31.3	88.7	37.6	–36.0
THF / Hex[a]	93.9	83.0	50.0	3.0	25.0	91.2	52.1	–3.7

0.01 M Concentration

Solvent	ee_A (%)	ee_B (%)	*de* (%)	dr (X : 1)	yield lost (%)	r (%)	r_α (%)	r_β (%)
Dioxane	64.4	74.7	23.1	1.6	38.5	68.4	20.2	–38.5
DME	95.1	77.1	28.6	1.8	35.7	88.7	33.0	44.4
Et_2O[c]	-	-	-	-	-	-	-	-
Et_2O / Hex	93.2	80.5	53.4	3.3	23.3	90.2	55.9	–7.0
PhH	93.4	88.9	55.5	3.5	22.2	92.4	56.4	–35.1
PhF	82.4	88.3	20.0	1.5	40.0	84.8	18.5	–38.6
PhMe	94.5	82.8	56.5	3.6	21.7	92.0	58.6	–7.0
PhMe / Hex	95.1	87.1	59.2	3.9	20.4	93.5	60.5	–19.4
t-BuOMe	95.1	90.3	47.4	2.8	26.3	93.8	48.3	–17.2
THF[a]	92.4	90.8	33.3	2.0	33.3	91.9	33.7	–24.6
THF[b]	95.7	90.5	33.3	2.0	33.3	94.0	34.5	5.0
THF / Hex[a]	95.7	81.0	45.9	2.7	27.0	91.5	49.2	26.3

[a] The THF employed in these reactions was dried by passing the solvent over a column of activated alumina with an argon overpressure. [b] The THF employed in these reactions was dried via distillation over benzophenone and sodium metal. [c] This reaction failed to afford measurable quantities of product.

3.6 NOTES AND REFERENCES

(1) Enquist, J. A., Jr.; Stoltz, B. M. *Nature* **2008**, *453*, 1228–1231.

(2) See chapter 2 for a thorough explaination of our synthetic endeavors toward the cyanthiwigin natural products.

(3) Mohr, J. T.; Behenna, D. C.; Harned, A. M.; Stoltz, B. M. *Angew. Chem., Int. Ed.* **2005**, *44*, 6924–6927.

(4) The value of ee_B is defined as the enantiomeric excess of the minor diastereomer of a double asymmetric transformation. If the minor diastereomer of such a reaction is *meso* in nature, this value is equal to zero under all conditions.

(5) (a) Langenbeck, W.; Triem, G. *Z. Phys. Chem. A* **1936**, *117*, 401–409. (b) Heller, D.; Drexler, H.-J.; Fischer, C.; Buschmann, H.; Baumann, W.; Heller, B. *Angew. Chem., Int. Ed.* **2000**, *39*, 495–499.

(6) Vigneron, J. P.; Dhaenens, M.; Horeau, A. *Tetrahedron Lett.* **1973**, *29*, 1055–1059.

(7) The intial yield, as well as the method of saponification of the carbonate species, was not specified.

(8) The value of diastereomeric exccess (*de*) is employed in place of dr for these graphical representations to achieve a scale comparable to *ee*. While calculated

values for dr range between zero and infinity, *de* varies only between zero and unity for the situations we consider. The value of *de* is calculated similarly to *ee*, and can be represented as the difference between the quantities of major and minor diastereomer produce, divided by the total material affored by the reaction:

$$de = \frac{[\text{Quantity of major diastereomer} - \text{quantity of minor diastereomer}]}{[\text{Quantity of major diastereomer} + \text{quantity of minor diastereomer}]}$$

(9) (a) Mori, K.; Tanida, K. *Tetrahedron* **1981**, *37*, 3221–3225. (b) Mori, K.; Watanabe, H. *Tetrahedron* **1986**, *42*, 295–304.

(10) Isaksson, R.; Liljefors, T.; Reinholdsson, P. *J. Chem. Soc., Chem. Commun.* **1984**, *3*, 137–138.

(11) Han, X.; Corey, E. J. *Org. Lett.* **1999**, *1*, 1871–1872.

(12) (a) Brown, H. C.; Singaram, B. *J. Org. Chem.* **1984**, *49*, 945–947. (b) Mathre, D. J.; Thompson, A. S.; Douglas, A. W.; Hoogsteen, J.; Carroll, J. D.; Corley, E. G.; Grabowki, E. J. *J. Org. Chem.* **1993**, *58*, 2880–2888. (c) Schwink, L.; Knochel, P. *Chem. Eur. J.* **1998**, *4*, 950–968.

(13) (a) Jadhav, P. K.; Prasad, J. V. N. V.; Brown, H. C. *J. Org. Chem.* **1985**, *50*, 3203–3206. (b) Toda, F.; Tanaka, K. *Chem. Lett.* **1986**, 1905–1908. (c) Brown, H. C.; Joshi, N. N. *J. Org. Chem.* **1988**, *53*, 4059–4062. (d) Venkatraman, L.; Periasamy, M. *Tetrahedron: Asymm.* **1996**, *7*, 2471–2474. (e) Periasamy, M; Venkatraman, L.; Thomas, K. R. J. *J. Org. Chem.* **1997**, *62*, 4302–4306.

(14) (a) Reuben, J. *J. Am. Chem. Soc.* **1980**, *102*, 2232–2237. (b) Feringa, B. L.; Smaardijk, A.; Wynberg, H. *J. Am. Chem. Soc.* **1985**, *107*, 4798–4799. (c) Pasquier, M.; Marty, W. *Angew. Chem., Int. Ed. Engl.* **1985**, *24*, 315–316. (d) Feringa, B. L.; Strijtveen, B.; Kellogg, R. M. *J. Org. Chem.* **1986**, *51*, 5485–5489. (e) Feringa, B. L. *J. Chem. Soc., Chem. Commun.* **1987**, 695–696. (f) Ouryupin, A. B.; Kadyko, M. I.; Petrovskii, P. V.; Fedin, E. I. *Chirality* **1994**, *6*, 1–4. (g) Platzer, N.; Rudler, H.; Alvarez, C.; Barkaoui, L.; Denise, B.; Goasdoué, N.; Rager, M.-N.; Vaissermann, J.; Daran, J.-C. *Bull. Soc. Chim. Fr.* **1995**, *132*, 95–113. (h) Hulst, R.; Kellogg, R. M.; Feringa, B. L. *Recl. Trav. Chim. Pay-B.* **1995**, *114*, 115–138. (i) Grotjahn, D. B.; Joubran, C. *Tetrahedron: Asymm.* **1995**, *6*, 745–752. (j) Cawley, A.; Duxbury, J. P.; Kee, T. P. *Tetrahedron: Asymm.* **1998**, *9*, 1947–1949. (k) Laverde, A., Jr.; Miranda, D. S.; Conceição, G. J. A.; Schirmer, H.; Pilli, R. A.; Meijere, A.; Marsaioli, A. J. *J. Brazil Chem. Soc.* **1999**, *10*, 293–298.

(15) Lagasse, F.; Tsukamoto, M.; Welch, C. J.; Kagan, H. B. *J. Am. Chem. Soc.* **2003**, *125*, 7490–7491.

(16) The following publication is the source of all mathmatical expressions in this section, with the exception of equations (11), (12), and (13): Baba, S. E.; Sartor, K.; Poulin, J.-C.; Kagan, H. *Bull. Soc. Chim. Fr.* **1994**, *131*, 525–533.

(17) In the following section, the configuration of each stereocenter for the isomers presented is represented in the format [1*P*, 2*P*], [1*S*, 2*S*], [1*R*, 2*R*], etc., for all possible combinations. The leading number (1 or 2) denotes the position of the

stereocenter as corresponding to either olefin (1) or (2) as shown in Scheme 3.10. The trailing letter corresponds to the configuration of that stereocenter as either *R* or *S*. Those centers referred to as *P* are prochiral, and have yet to undergo transformation.

(18) In the examples provided, the enantioselective catalyst employed is arbitrarily assumed to favor generation of the *R* enantiomer at each reactive center.

(19) The graphical representations depicted in Figure 3.2 utilize an expression for dr which has been converted to *de* in order to keep the scale of the curves consistant.

(20) For an alternative mathematical treatment of this system that reaches the same conclusion, see: Soai, K.; Hori, H.; Kawahara, M. *J. Chem. Soc., Chem. Commun.* **1992**, 106–108.

(21) The relationship between the enantiomeric excess of the minor diastereomer (ee_B) and either selectivity term can also be plotted. In this case, the value of ee_B varies between 1 and –1, indicating that the minor diastereomer can yield either sense of enantiomeric product depending upon the dominance of either the r_1 or r_2 term. Interestingly, the magnitude of the r terms alone does not dictate the final value of ee_B. Instead, the determining factor is the overall difference between the values of r_1 and r_2. Under all conditions where both r_1 and r_2 are equal, ee_B will be zero. If r_1 and r_2 are very close in value, ee_B will be very small. Only in situations where a large disparity exists between r_1 and r_2 will ee_B display a correspondingly large

value. In contrast to the behavior of ee_A, under no circumstances will ee_B ever exceed the value of either r_1 or r_2.

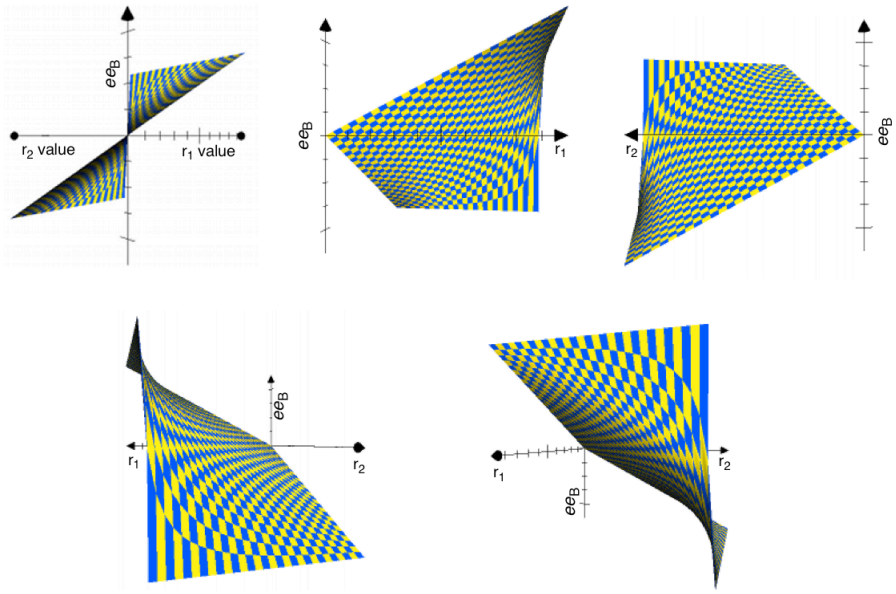

(22) Taylor, M. S.; Jacobsen, E. N. *Pro. Natl. Acad. Sci. U.S.A.* **2004**, *101*, 5368–5373.

(23) Examples of multiple stereoselective catalysis in which five or more stereocenters are set simultaneously have been reported. Though the general trends in enantioselectivity and diastereoselectivity are the same as observed in double asymmetric transformations, the mathematically complex nature of these reactions precludes a rigorous treatment here.

(24) For examples of multiple asymmetric processes that are not related to total synthetic efforts, see: (a) Hoye, T. R.; Suhadolnik, J. C. *Tetrahedron* **1986**, *42*, 2855–2862. (b) Crispino, G. A.; Sharpless, K. B. *Tetrahedron Letters* **1992**, *33*,

4273–4274. (c) Crispino, G. A.; Ho, P. T.; Sharpless, K. B. *Science* **1993**, *259*, 64–65.

(25) Lebsack, A. D.; Link, J. T.; Overman, L. E.; Steams, B. A. *J. Am. Chem. Soc.* **2002**, *124*, 9008–9009.

(26) Xiong, Z.; Corey, E. J. *J. Am. Chem. Soc.* **2000**, *122*, 9328–9329.

(27) Wang, Z.-X.; Tu, Y.; Frohn, M.; Zhang, J.-R.; Shi, Y. *J. Am. Chem. Soc.* **1997**, *119*, 11224–11235.

(28) Xiong, Z.; Busch, R.; Corey, E. J. *Org. Lett.* **2010,** *12*, 1512–1514.

(29) The alkylation of either substrate **189** or **233** is unlikely to involve a discrete ketone enolate. In spite of this, intermediates **277–280** are depicted in this manner in order to provide a schematic representation of the reaction course.

(30) This experiment was run with a 1 : 1 mixture of diastereomers of **287** as the starting material, and was also repeated twice more with either pure diastereomer of **287**. In all three reactions, the results obtained showed a dr in excess of 50 : 1 regardless of the starting diastereomer employed.

(31) In this case, the negative value obtained for the r term is assigned via relative comparison to the diastereomers observed in the (*S*)-*t*-BuPHOX case.

(32) To see the results of all 48 experiments in this screen, please see the experimental section of this chapter.

(33) (a) Helmchen, G.; Pfaltz, A. *Acc. Chem. Res.* **2000**, *33*, 336–345. (b) Tani, K.; Behenna, D. C.; McFadden, R. M.; Stoltz, B. M. *Org. Lett.* **2007**, *9*, 2529–2531.

(34) Peer, M.; de Jong, J. C.; Kiefer, M.; Langer, T.; Rieck, H.; Schell, H.; Sennhenn, P.; Sprinz, J.; Steinhagen, H.; Wiese, B.; Helmchen, G. *Tetrahedron* **1996**, *52*, 7547–7583.